Old Dominion University

ODU Digital Commons

Mechanical & Aerospace Engineering Theses & Dissertations

Mechanical & Aerospace Engineering

Spring 2020

Through-Thickness Reinforcement and Repair of Carbon Fiber Based Honeycomb Structures Under Flexure and Tension of Adhesively Bonded Joints

Aleric Alden Sanders
Old Dominion University, mathlete229@gmail.com

THROUGH-THICKNESS REINFORCEMENT AND REPAIR OF CARBON FIBER BASED HONEYCOMB

STRUCTURES UNDER FLEXURE AND TENSION OF ADHESIVELY BONDED JOINTS

by

Aleric Alden Sanders
B.S.M.E May 2018, Old Dominion University

A Thesis Submitted to the Faculty of
Old Dominion University in Partial Fulfillment of the
Requirements for the Degree of

MASTER OF SCIENCE

MECHANICAL ENGINEERING

OLD DOMINION UNIVERSITY
May 2020

Approved by:

Oleksandr G. Kravchenko (Director)

Krishna Kaipa (Member)

Dipankar Ghosh (Member)

Andrew Bergan (Member)

ABSTRACT

THROUGH-THICKNESS REINFORCEMENT AND REPAIR OF CARBON FIBER BASED HONEYCOMB
STRUCTURES UNDER FLEXURE AND TENSION OF ADHESIVELY BONDED JOINTS

Aleric Alden Sanders
Old Dominion University, 2020
Director: Dr. Oleksandr G. Kravchenko

Repair and reinforcement of composite honeycomb structures is an area of concern as
higher demands are being placed on high strength, lightweight structural materials, such as
carbon fiber reinforced plastics and corresponding honeycomb structures. A common issue with
these structures is when a delamination in the facesheet may form and spread, leading to a
failure scenario. An investigation of adding a through thickness reinforcement (TTR) to these
structures at the sample level that undergo four-point-bending, tension, and joining methods is
conducted throughout this thesis. The embedding of pultruded carbon fiber rods is found to be
an ideal addition to composite honeycomb structures, not only in terms of reinforcement but
also for repair and damage isolation. Facesheet thickness is found to play and important role in
the effectiveness of TTR in four-point-bending. Adhesively bonded joints are tested to failure
and the addition of defects and TTR are used to further analyze the potential failures of double
lap joints in composite structures and how TTR may help to minimize damage in those scenarios.

This thesis is dedicated to my parents, who have been with me along every step of life's journey to this point. They have helped me greatly through means of character development, decision making, and financial needs. This paper sums up my year and a half of work in the composites field, an opportunity I was only able to take because of their love and support for me.

This paper is also dedicated to my fiancée, Kendal. The completion of my thesis and Master's degree is a pivotal moment in my life where I have a shift in focus from the schooling career I started as a child to a mechanical engineering career, where I will no longer work for the gain of myself, but for my family.

I would also like to recognize those individuals and groups who helped me with my research in the Composites Modeling and Manufacturing group (CCM), specifically Manjukrishna Suresh and Austin Brittingham. These two individuals were there for me in the manufacturing and testing phases, as many tasks require more than one person. Thank you both.

AKNOWLEDGEMENTS

First and foremost, Dr. Oleksandr "Alex" Kravchenko has been the best advisor possible to me from the beginning. When a project in the making fell through over the summer of 2018 between myself and another professor, Dr. Kravchenko was there to lend a hand and put me on a path to success. Since starting my journey in composites research, I have been entrusted with many expensive pieces of equipment and the amount of support and willingness to see my crazy ideas out means a lot. Working with Dr. Kravchenko not only has given me the opportunity to learn about composites in great depth, but to learn more about myself. Over the past year and a half, I have challenged my abilities, gained greater confidence, and developed in my professionalism through presentations and participation in the 2019 SPE ACCE conference.

To Dr. Bawab and the ODU Department of Mechanical and Aerospace Engineering, thank you very much for having the facilities and funding to make such a high level of research possible. I greatly appreciate the support I was provided, not only monetarily through stipends, but also in the education in your curriculum and in hands-on programs, particularly the Society of Automotive Engineers (SAE), that helped me to grow as an engineer.

TABLE OF CONTENTS

Page

LIST OF TABLES

LIST OF FIGURES

Figure   Page

Figure   Page

Figure   Page

Figure   Page

INTRODUCTION

The demand for strong, lightweight materials and structures is on the rise. With new advancements in materials and technology, the limit of what is physically possible continues to be questioned and taken to the next level. One of these technologies is composite structures, which is relatively new when considering man's understanding of other materials for thousands of years. For example, the use of concrete dates to 6500 BC, and mankind has since advanced the formulations, shapes of structures, and combination with other materials, namely rebar, to build structures that weren't imaginable only 100 years ago.[1] Concrete, however, is not a lightweight material, and it is only ideal when used in compression. It is an excellent example of a composite material that has been around for a long time and has had the opportunity to be advanced to what it is today.

A relatively new composite that has excelled in many industries recently is carbon fiber reinforced polymers. This class of materials is found to perform very well under tensile and compressive loads for many industry applications. It is also lightweight, making it an ideal material for many scenarios where mass, efficiency, or acceleration is a concern. Because carbon fiber has not been around nearly as long as concrete, there are still many questions regarding its capabilities. Carbon fiber may seem like an ideal material for many of today's engineering problems; however, the questions regarding the repair of composite structures must be further understood.

It was not until 1860 that the first carbon fibers were produced.[2] These fibers were primarily used in lightbulbs, as a much lower carbon percentage was present in these fibers

compared to the fibers of today. It would be another 100 years until this material was primarily used the way we know it to be today in the reinforcement of composite structures.[3]

The use of carbon fiber in composite structures primarily began in the aerospace industry, as supply was low and cost was high.[4] As is the case with most modern technology, there is a trickle-down effect, where the consumer demand goes up, driving the supply up and the cost down. Advancements in manufacturing methods also affect the cost, as many companies research the best ways to produce carbon fiber composite structures at a competitive cost for the consumer market. Once considered to be spaceship technology, carbon fiber is finding its way to products that everyday people use, from automobiles to eyeglasses.

With the expansion of uses of any material comes the desire to not only manufacture the product cheaper but to also enhance the quality and properties of the given product. With more uses of carbon fiber comes more challenges for the material. The limits are explored more frequently and to a greater extent in the name of efficiency and design optimization. While basic material properties of carbon fiber composite structures are greatly understood and can be accurately modeled in computer simulation software, there is still the need for experimentation of some of the material's weak points. Attempts have been made to eliminate some of carbon fiber's shortcomings, primarily in its tendency to fail at lower loads when in bending and to fracture beyond repair.

A great way to increase the bending stiffness and reduce the bending stresses on a carbon fiber laminate structure is to design the layup into a sandwich, where the carbon fiber laminate will be present on the outsides of the sandwich (often called a facesheet) and the center will be composed of a lightweight solid material that allows for easy bonding (often foam or a

honeycomb structure of aluminum or aramid with phenolic resin material known as Nomex).[5] Chemical and heat resistance can also play a factor in core material selection, as composite sandwich structures are often exposed to harsh environments.[6] The thicker the core, the higher the capable bending stiffness due to the I-beam effect.[7] This configuration allows for one side of the structure to be in compression while the other side is in tension, both of which are properties that carbon fiber excels in.[8]

While sandwich panels help in keeping the loads in the axial direction of the fibers, there are still issues with disbonds and delaminations that can occur either in the fabrication or loading phases, especially after many cycles.[9] There have been a few proposed methods to help mitigate this problem and to repair or reinforce troublesome regions on composite honeycomb parts. This thesis will look into these methods in the background section and will more specifically investigate the through thickness reinforcement (TTR) method of repair and reinforcement for structures exposed to four-point bending and tension loads.

BACKGROUND OF THE STUDY

In February of 1992, the Boeing Military Airplanes Division published a paper on z-pinning of composite laminates at the Aerospace Design Conference in Irvine, California. The study placed graphite / epoxy pins (z-pins) in a foam core sandwich layup, perpendicular and through the planes of the facesheet before the curing process. Once cured by an autoclave, the samples were tested in harsh environments designed to simulate elements that an airplane wing and body would be exposed to. A double cantilever beam (DCB) test was also conducted to understand the enhanced resistance to fracture that z-pinning added to the composite. The conclusions of the study were positive, in that there was an increase in fracture resistance in the DCB test and the delaminations were fewer and of smaller magnitude in tests that simulated hail and ballistic rounds.[10] The intention of this investigation was to come up with a lightweight solution to the reinforcement of aviation composite structures and was deemed successful, but it never seemed to take off in production, likely due to the increased complexity of the manufacturing process.

Another study on this topic was conducted in 2005 on the fabrication of composite T-joints, where the addition of z-pins and tufting was performed on the samples in order to study the difference in loading capabilities and crack propagation. For the pinning method of reinforcement, T-joints were made of unidirectional carbon fiber prepreg and the z-pins were inserted by careful placement of the cured carbon fiber rods in a foam, then pushed into the prepreg through the use of an ultrasonic horn. In the tufting method, a dry fabric was used in the making of the T-joints due to the ease of running the joint through a stitching machine avoiding the mess and stickiness of resin, which was infused into the fibers following the tufting

process. While testing and modeling proved the tufting method to be more effective than z-pinning due to the tendency for the thread to hold the fibers together better without pulling out, both methods were deemed effective in that their capable loads were significantly higher than that of the unreinforced control. Tufting was also praised for its ease of manufacturability compared to z-pinning.[11]

A revised method to z-pinning is through thickness reinforcement (TTR), where instead of adding the cured carbon fiber rods before the laminate curing process, tiny holes are drilled into the composite post-cure and the rods are inserted along with resin. A published paper by Dr. Kravchenko from 2013 investigates this idea and tests the fracture resistance in mode I DCB testing, just as Boeing did in its paper previously discussed. The use of this alternate method over z-pinning was desirable for ultimately improving fiber alignment. Due to this reinforcement method taking place on a sample that would be considered pristine initially, the fibers are aligned as best as possible in the manufacturing process; then some fibers are drilled through where the reinforcement is to be present. This allows for the fibers around the reinforcement to be ideally aligned. Through the increase in critical possible load and corresponding displacement, it was found that the effective fracture toughness of composite laminate can double in mode I DCB testing before sample failure and crack propagation. Different placement of reinforcement from the edge was also tested and found to be significant in terms of stiffness, response, and load improvement.[12] Further studies conducted by Dr. Kravchenko also look into the aspect ratio (AR) of the embedded rod and analyze the increase of resiliency with the increase of the AR.[13]

In an effort to apply through thickness reinforcement to common composite structures, a 2019 study applies TTR to carbon fiber honeycomb structures and tests them in four- point

bending. Defects were also applied to these samples, as PTFE (Teflon) inserts to simulate delaminations and disbonds were added into the layups in the region of maximum bending moment. Some crack propagation was observed in the defected samples, which was suppressed when TTR was applied to the area of concern. This study not only focused on the reinforcement aspect of the TTR method but also the repair aspect. Testing showed that the defected samples were significantly weaker than the pristine samples, but when TTR was added, either in repair or in reinforcement, the load capacity was on par with or surpassed that of the pristine samples.[14] This paper will look closely into this specific problem and will change the facesheet material to a unidirectional prepreg in order to have an enhanced crack propagation in need of suppressing.

Then this paper will investigate a problem introduced by enabling damage tolerance to adhesively bonded joints. The adhesive joints for composite structures have been considered by the National Aeronautics and Space Administration (NASA) in one of its future space structures design of Space Launch System. Specifically, a large conical structure made of a carbon fiber honeycomb construction was designed to take up the entire diameter of a spaceship and allow for a strong, stiff, and lightweight separation between the upper exploratory stage and the payload (Figure 1). This structure is ideally manufactured as one piece in an autoclave; however, due to limitations in manufacturability and fabrication, this structure will be made in eight separate pieces and joined together through use of a double lap joint method. The idea is to set a small gap between two of the pieces and join that gap with layers of adhesively bonded carbon fiber plies, connecting the facesheets on both sides of the honeycomb composite structures. NASA conducted many tests on this fabrication method, making these joints at the sample level and testing them in tension while also validating the results with computer models. Results

proved to be successful, as the designed joint was capable of withstanding loads more than five times the design limit and the computer models were able to accurately predict the failure load within 10 to 15 percent.[15]
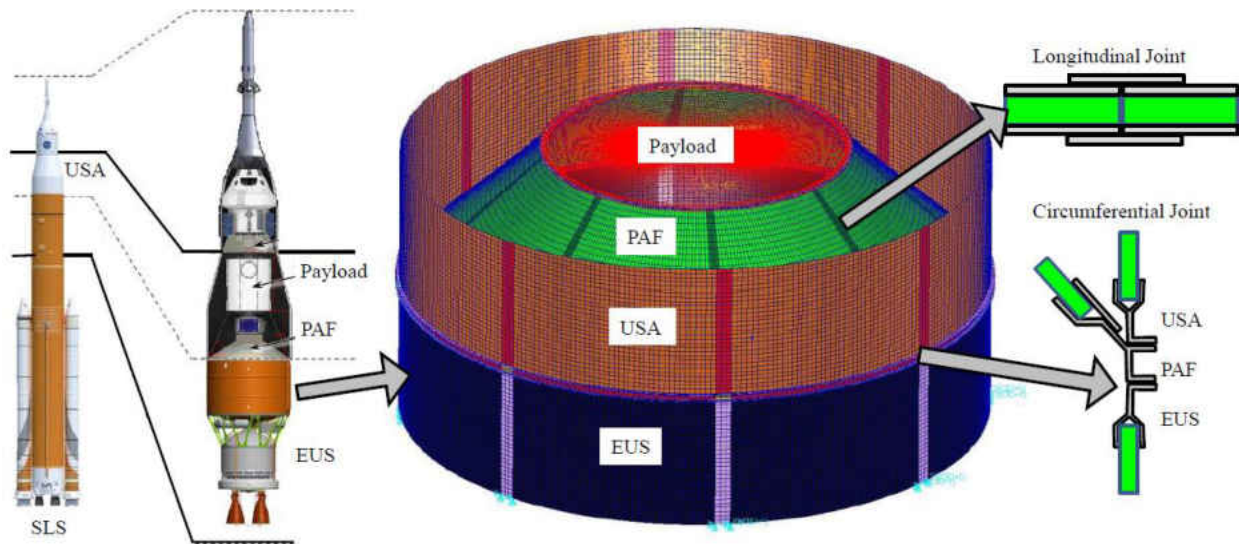
Figure 1: NASA's exploded view of the payload attachment fitting and joints

Regarding lap joints and their effectiveness in joining, extensive research has been conducted in the design of the joint and the amount of adhesive that is required for maximized strength and stress distribution. A 2015 study performed in Portugal concludes that there are four key attributes to a lap joint that will enhance its performance: the adhesive must have a low modulus of strength and high ductility, similar materials should also be used on both sides of the bond, the adhesive layer should be thin, and the surface area for adhesion should be maximized.[16]

Other methods of joining and repair include scarfing and a stepped lap. In a scarf repair, a diagonal of the cross section of the composite structure is cut, where a complementing diagonal

is adhesively bonded to the cut. A stepped lap joint combines the attributes of a lap joint and a scarf repair, where the "steps" are formed by overlapping composite plies and are adhered to matching steps at the location of repair (Figure 2). These two methods of repair are more predominate in composite structures with a significant thickness that will allow for a sizable surface area for adhesion.[17]
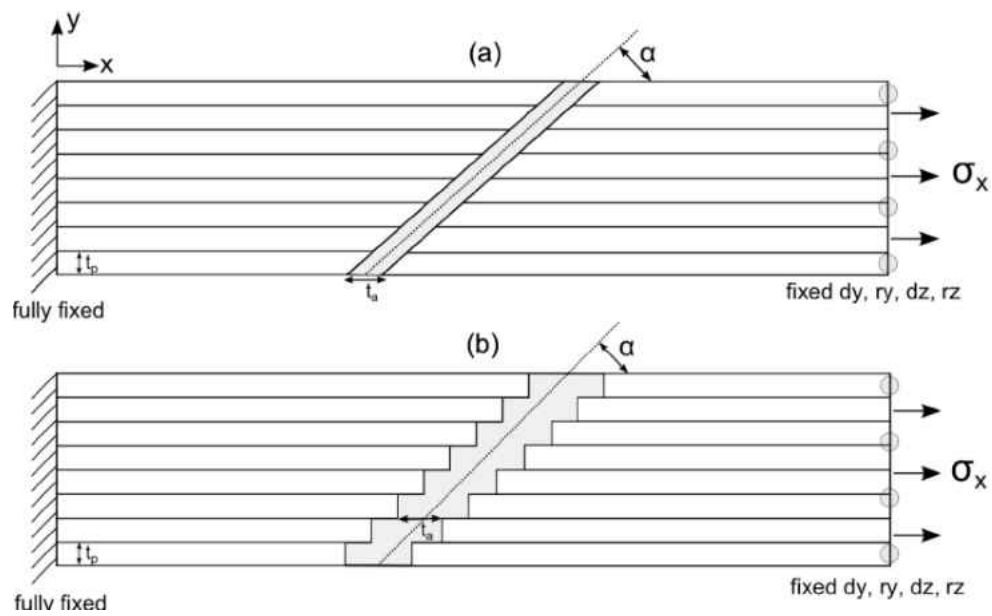
Figure 2: Design parameters for (a) tapered scarf joint, and (b) stepped-lap joint

FOUR-POINT BENDING METHODOLOGY

As an extension of Manjukrishna Suresh's research, there was particular interest in the effect of TTR in pristine, disbonded, and delaminated samples in four-point bending with a unidirectional layup. The important difference is in the change of properties between a weave and unidirectional ply of carbon fiber. The unidirectional ply is more brittle and is therefore more likely to fail in a manner with significant crack propagation when compared to the weave pattern. Another area of interest was in the thickness of the facesheet and how that might change the effectiveness of the TTR repair or reinforcement.

The design and fabrication of the unidirectional carbon fiber honeycomb samples shares an almost identical design with Mr. Suresh's samples, as each sample will be cut from a plate, where a cured plate allows for fabrication of five samples. Four or eight plies make up a facesheet (two versions of samples were made), as these facesheets are bonded to a 0.460" thick Nomex honeycomb core with an adhesive film (Figure 3). Each sample will measure approximately one inch wide by 21 inches in length. The span of the four-point bending test is 20 inches, and the rollers will allow for a maximum bending moment at the center three inches (Figure 4). The disbond and delamination defects are formed by a thin polytetrafluoroethylene (PTFE) Teflon strip in the top facesheet, applied to the center inch of the sample lengthwise and inserted either between the adhesive film and bottom ply or between the second and third plies, respectively.
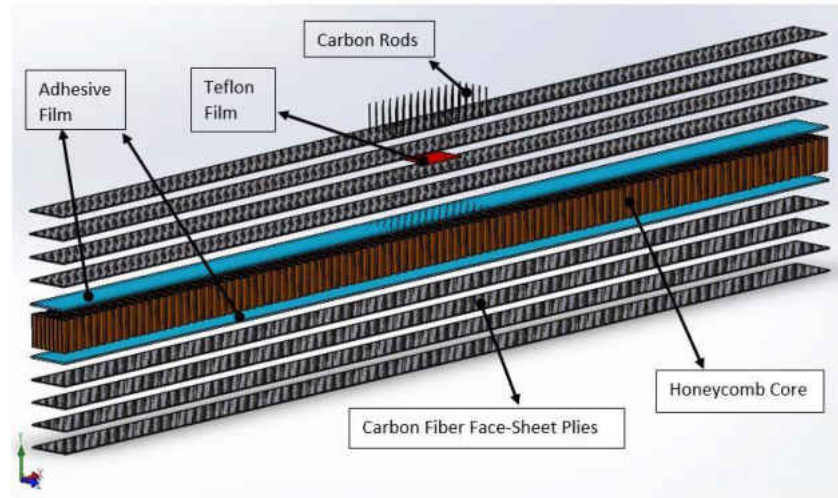
Figure 3: Four-point-bending sample configuration 3D model
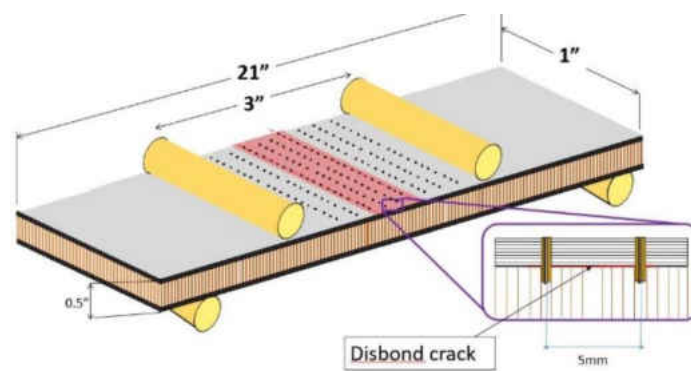
Figure 4: Four-point-bending test dimensions

The materials required for fabrication included two aluminum plates to be used as tools (top and bottom tools), tacky tape, vacuum bagging sheet, high temperature peel ply, breather material, flash tape, a vacuum port, and the raw supplies (unidirectional carbon fiber prepreg from Fibreglast, Nomex honeycomb from Rock West Composites, Loctite EA 9696 epoxy adhesive film, and teflon) (Figure 5). The equipment used in fabrication included a vacuum pump and Wabash Genesis series heat press. (Figures 6)

(a)   (b)

Figure 5: Fabrication process: (a) layup of sandwich panel and (b) vacuum bagged panel

(a)   (b)

Figure 6: Curing process: (a) Heat press (front) and (b) heat press (rear)

The curing process included multiple steps, where temperatures and pressures were chosen from literature and product data sheets. The first curing stage goes up to a temperature

of 80˚C and a pressure of 15psi while under vacuum. This is to decrease the viscosity of the resin and allow excess resin to bleed while removing voids and volatiles.[18] The second stage curing temperature was chosen to be 130˚C due to the data of both the adhesive film and prepreg having overlapping curing temperatures.[19][20]

There were three different types of manufactured plates, as each plate was either pristine, disbonded, or delaminated. Each plate was then cut into five samples lengthwise, as the center 6.2” x 21” were of concern and the edge effect on all four sides were cut off, as the plates were oversized. Cutting was performed through the use of an OMAX ProtoMAX waterjet cutting machine.   A 1.040” separated each cut, as the machine is accurate with position to the thousandth of an inch, and 40 thousandths of an inch was found through experimentation to be the cut thickness (Figure 7). Waterjet cutting provided many benefits in this stage of fabrication, as opposed to other conventional methods. Low heat, CNC capabilities, cleanliness, and safety are among the top reasons for this method of cutting. A disadvantage with this specific machine is that its cutting limitations are on a 12” x 12” platform. This did not prove to be too great of an issue, given the size of an object that could be laid flat in the machine is approximately 24” x 14”. Once all the cutting was performed from one side to just over the half-way point, the plate was simply flipped around and aligned with the cutting path so that the five samples could have the second half of the cutting completed.

Figure 7: Waterjet cutting of a panel

Following the cutting process, the samples are then allowed to dry in an oven at 110˚C and then cleaned with acetone to wipe off an abrasive dust left by the waterjet. At this point TTR is applied to the necessary samples. For the first round of testing of a given batch, three samples are tested in an "as is" condition and the remaining two have TTR reinforcement. The samples without TTR for the disbonded and delaminated batches are tested to initial failure, meaning the test concludes if there is a sudden drop in load or propagation of a crack. The goal is to catch the sample in its "failed, but repairable" state and apply TTR as a repair, rather than reinforcement before loading. See Figure 8 for the testing plan of the different samples. This plan was implemented for both four ply facesheet and eight ply facesheet versions of samples.
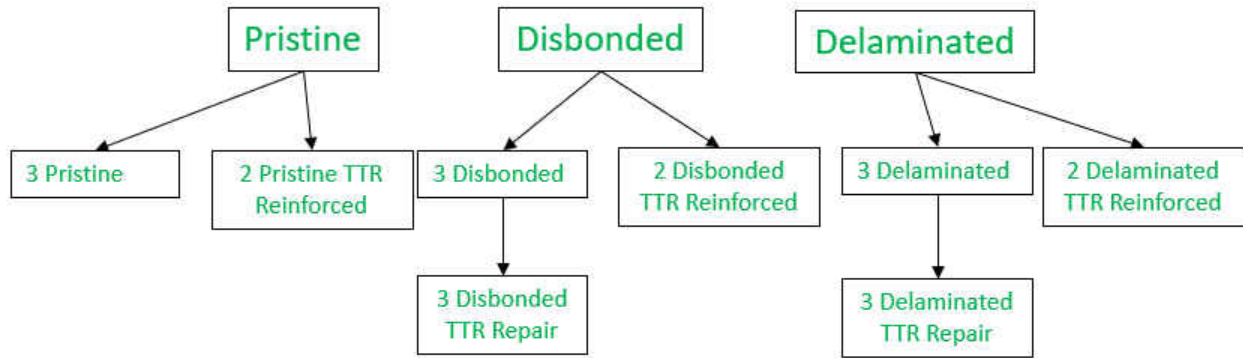
Figure 8: Fabrication and testing plan for four-point bending samples

The process of conducting through thickness reinforcement, either in a manner of repair or reinforcement is the same. In the center three inches of the sample, a grid pattern of 0.75mm holes are drilled through the facesheet in the area of concern with a rotary tool attached to a press, acting like a traditional drill press (Figure 9). Once these holes are drilled, the sample is cleared of the carbon / epoxy dust by blowing it off and then wiping it with acetone so that the epoxy can have an effective cure in a future step. At this point, 0.5mm pultruded carbon rods are cut to approximately 3/4" so that they may be placed in the drilled holes and allowed to stick out (it is better for the rods to be too long rather than too short). A good visualization of the placement of these rods is shown in Figure 10, where the carbon rods are acting as a repair on an eight ply facesheet sample with a delamination and propagated crack. Once the cut rods are in place, a two part epoxy is mixed and applied to the region, allowing for the bonding of the rod to the facesheet and honeycomb core (Figure 11). Once fully cured, the excess carbon rods and resin above the top surface of the facesheet are sanded down so that the repair may be better analyzed.

Figure 10: Drilling setup for TTR

Figure 9: TTR applied to critical area

Figure 11: TTR curing process

Prior to testing, a thin paint layer should be applied to all samples to measure strain via use of a digital image correlation (DIC) setup. When prepping the samples for use of the DIC, a light coating of matte black is sprayed onto the samples. If sprayed too thin, the sample is too reflective due to epoxy glare. If sprayed too thick, the top surface of the paint could be deforming in a different manner than the facesheet of the sample. On top of this matte black layer is a dusting of white paint. This dusting allows for a speckled pattern to be observed. The DIC software uses these speckles to create a surface and track its movement throughout the test. This allows for strain measurements to be made without the use of a traditional strain gauge.

Another advantage of the DIC is that more than one point is analyzed, in that continuous strain profiles on the surface can be observed and recorded. More capabilities of this equipment will be explained and visualized in the results section of this thesis.

At this point, the samples are ready to be tested. A Tinus Olsen tension / compression testing machine is used and an aluminum beam with supports for the samples is centered diagonally through the machine. This orientation allows for a DIC camera to be appropriately positioned for recording strain. With a 50mm lens on the DIC camera, the operating distance is 480mm. The camera should also be carefully positioned so that the image is as flat as possible at the region of concern, without allowing the four-point bend attachment to cast a shadow, as the DIC operates using light (Figure 12).

Testing was performed at a crosshead rate of 4mm per minute to achieve a static loading simulation. The data from the Tinus Olsen machine and the DIC software were recorded at a rate of 1Hz until sample failure occurred.
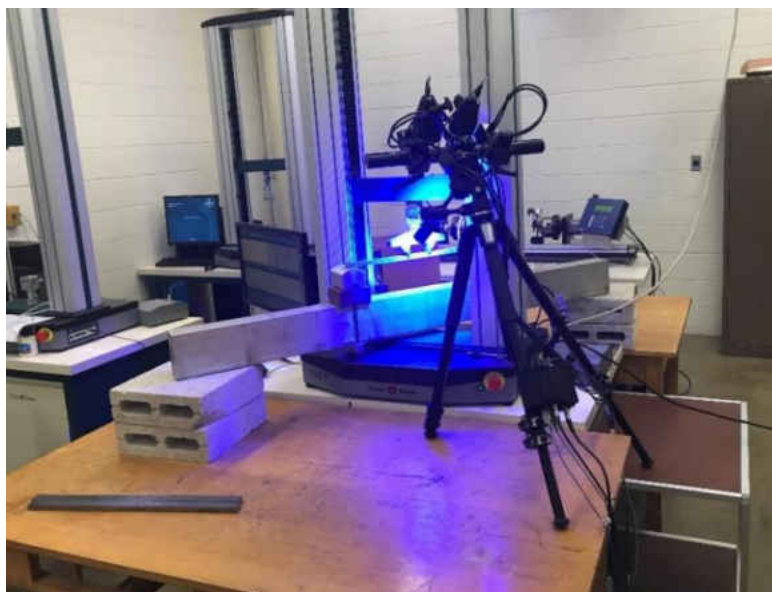
Figure 12: Four-point bending test setup

FOUR-POINT BENDING RESULTS

From the research of the woven facesheet samples of Mr. Suresh's study of the non-TTR samples, the pristine samples proved to have a higher load capacity, followed by the delaminated and then the disbonded samples. When TTR was applied to the weaker samples in the form of a repair, the results found that the delaminated and disbonded samples were able to have maximum load capabilities close to that of the pristine samples (Figure 13). To take matters a step further, TTR was applied to all sample types as a form of reinforcement (before being loaded), to which there was further improvement across all samples (Figure 14). The reinforced delaminated samples were even able to out-perform the reinforced pristine samples. Similar trends were to be expected in this experiment with unidirectional carbon fiber facesheets.
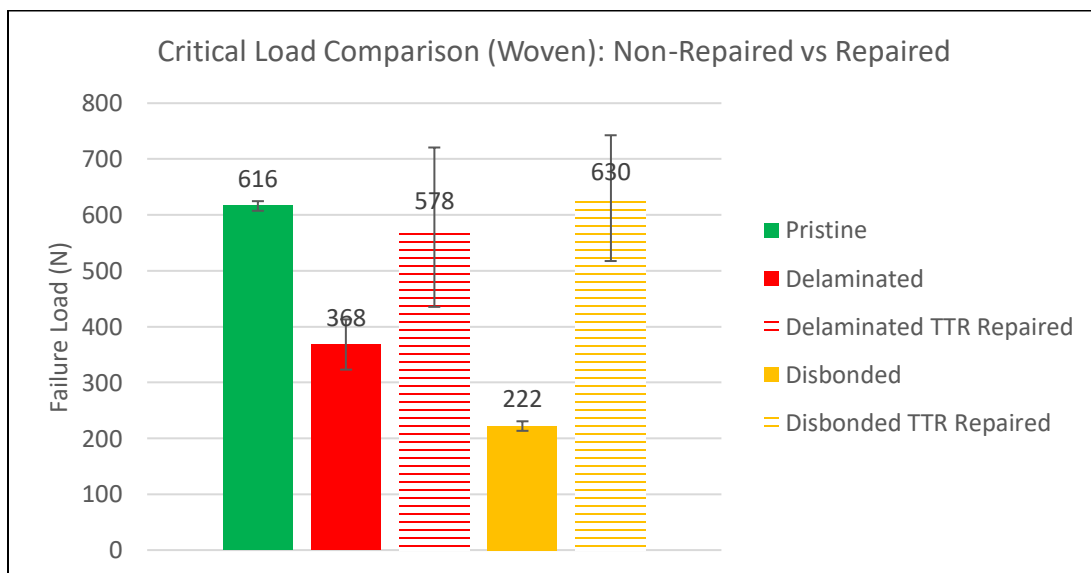
Figure 13: Mr. Suresh's comparison of non-repaired and repaired samples
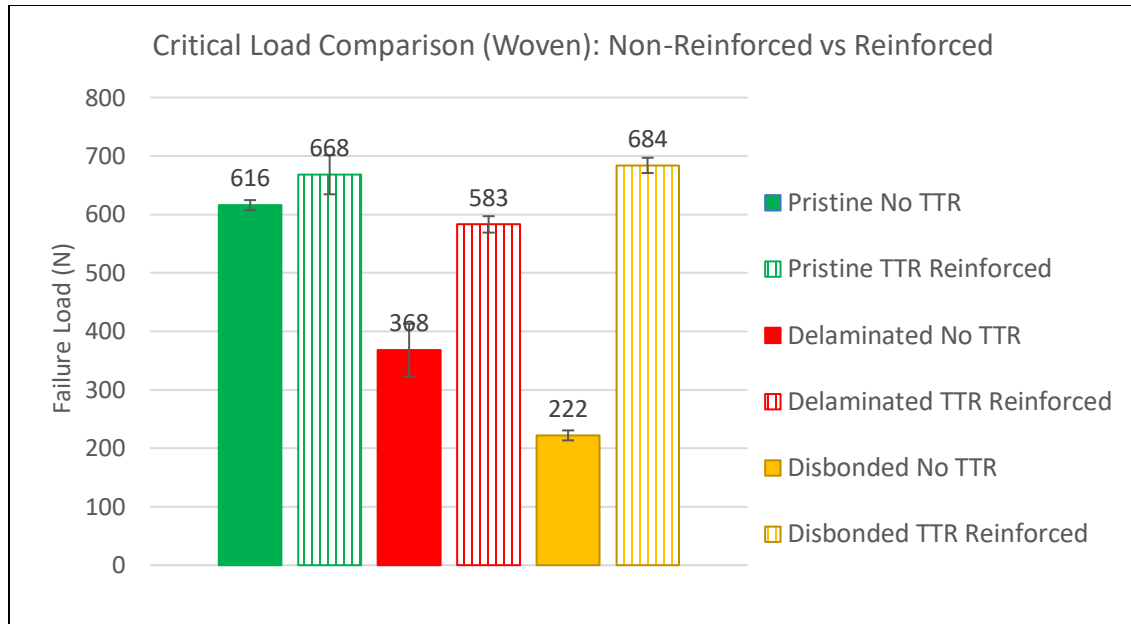
Figure 14: Mr. Suresh's comparison of non-reinforced and reinforced samples

After fabricating the four ply facesheet samples, conducting loading tests, and analyzing the data, a familiar trend that was different in magnitude was found. See Figures 15 and 16 for a direct comparison of the four ply facesheet samples to Mr. Suresh's charts. A very high pristine failure load value was found while all the other results remained much lower than the woven counterparts. The reason for this difference when compared to the woven prepreg isn't only in the orientation of the fibers but also in the thickness of the plies themselves, as a unidirectional ply used in this work is half the thickness of a woven ply.
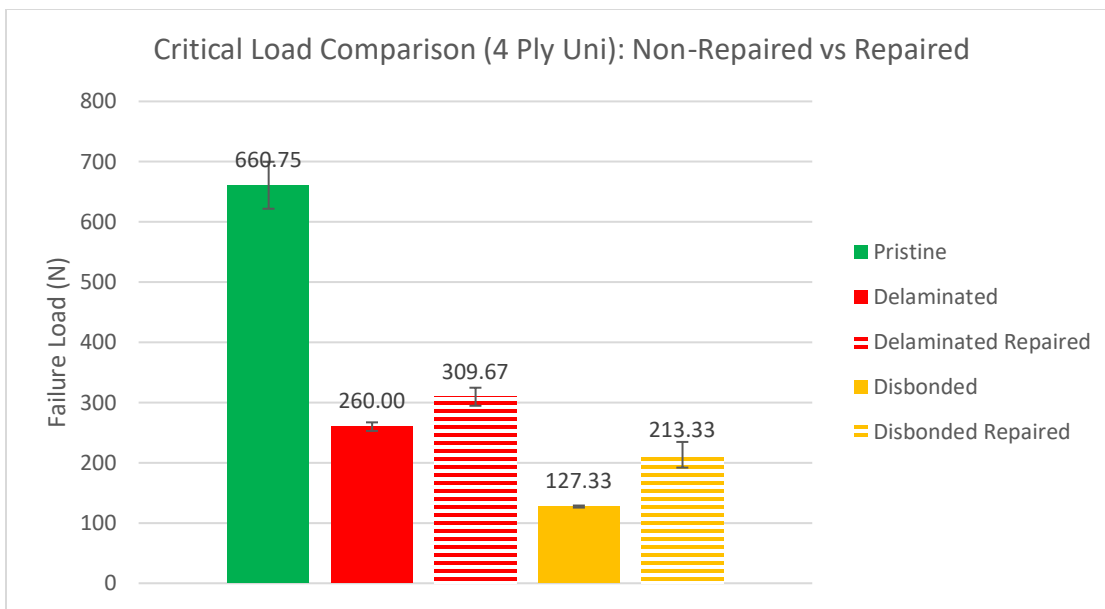
Figure 15: Comparison of unidirectional non-repaired and repaired four ply samples
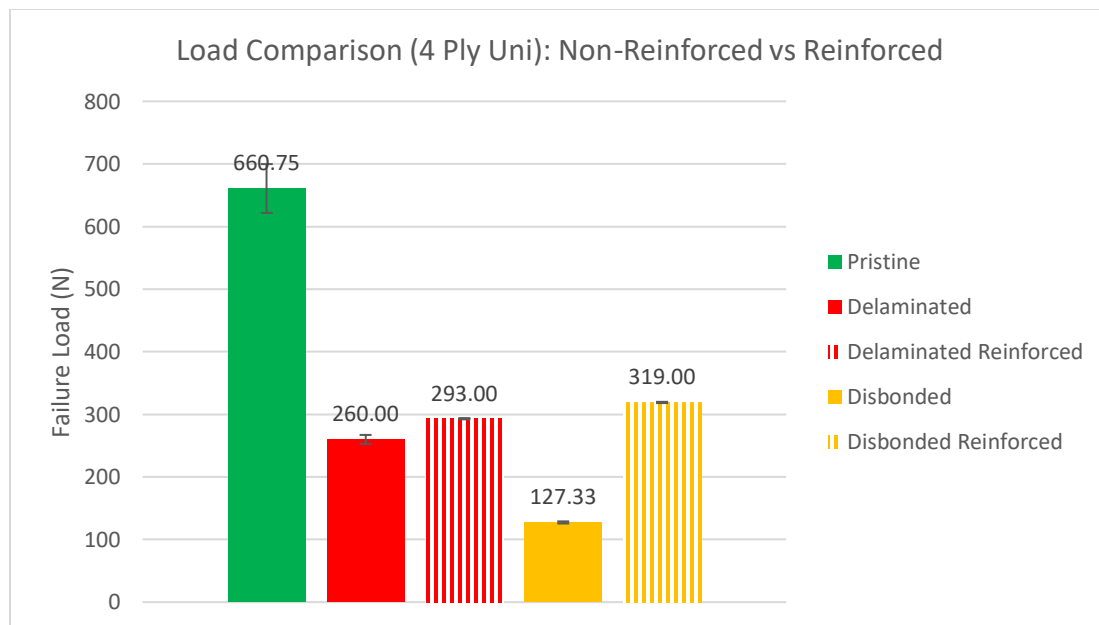
Figure 16: Comparison of unidirectional non-reinforced and reinforced four ply samples

This test was a success in that four ply facesheet samples had half the facesheet thickness as Mr. Suresh's study and were able to exert the same load carrying abilities in the pristine state.

The disbonded and delaminated samples had an enhanced failure mode, as the crack propagation not only began sooner but also spread across the region of maximum moment between the upper load application points.

Among the four ply delaminated and disbonded samples, a lower loading capability was observed, when compared to the woven defected samples. Additionally, the effectiveness of TTR dropped. Mr. Suresh observed a 57.1% and a 183.7% increase in load from the delaminated and disbonded samples, respectively, after repair. This test observed a 19.1% and a 63.5% increase, respectively, after repair. As predicted, the effectiveness of the repair was decreased as the thickness of the facesheet was decreased. In other words, the aspect ratio of the TTR rod was found to be an important factor as expected from previous studies.

To further explore the aspect ratio effect, the same lower percentages should be observed in the TTR Reinforced samples. Mr. Suresh observed a 58.4% and a 208.1% increase in load from the delaminated and disbonded samples, respectively, after reinforcement. This test observed a 12.7% and a 150.5% increase, respectively, after reinforcement. There was little change to the effectiveness of TTR in the repaired and reinforced delaminated samples while there was a noticeable increase in effectiveness of TTR in the repaired and reinforced disbonded samples. All four ply unidirectional effectiveness values were below that of Mr. Suresh's effectiveness values in both the repaired and reinforcement scenarios. The importance of this will be addressed in the conclusions section.

In regard to stiffness of the unidirectional samples, there was little deviation in the rate at which the force was applied at the set crosshead rate. This was true for all samples: pristine, defected, and with TTR. Across the board, the average stiffness value for each sample type was

between 22.7 and 25.4 N/mm. These readings were obtained through use of a built-in linear regression tool in Microsoft Excel and was applied to the most linear region of data in the Load vs Displacement graph of each sample. The stiffness of each sample can be determined and visualized by the slope of the load vs displacement curve. For reference, Mr. Suresh's samples were stiffer, at approximately 40 N/mm, as the facesheets of those samples were thicker. See Figures 17 and 18 for the load vs displacement curves of Mr. Suresh's studies and compare them to the results in this experiment as shown in Figures 19 and 20. A noticeable difference in slope and TTR effectiveness will be easy to identify.
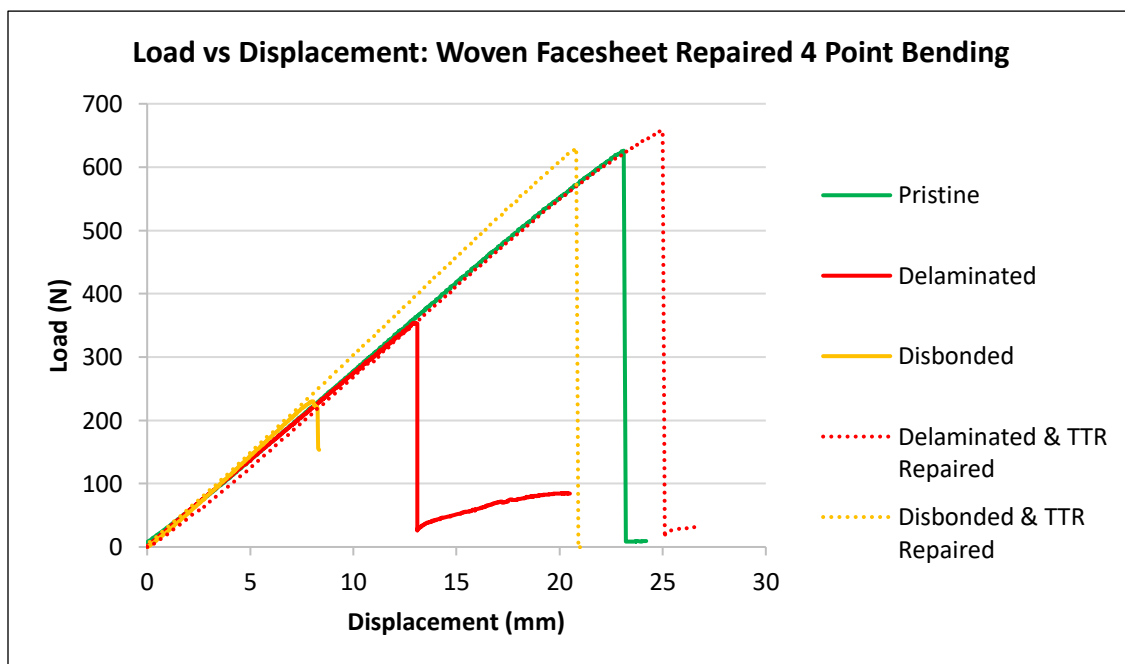
Figure 17: Mr. Suresh's graph comparison of TTR repaired samples to controls
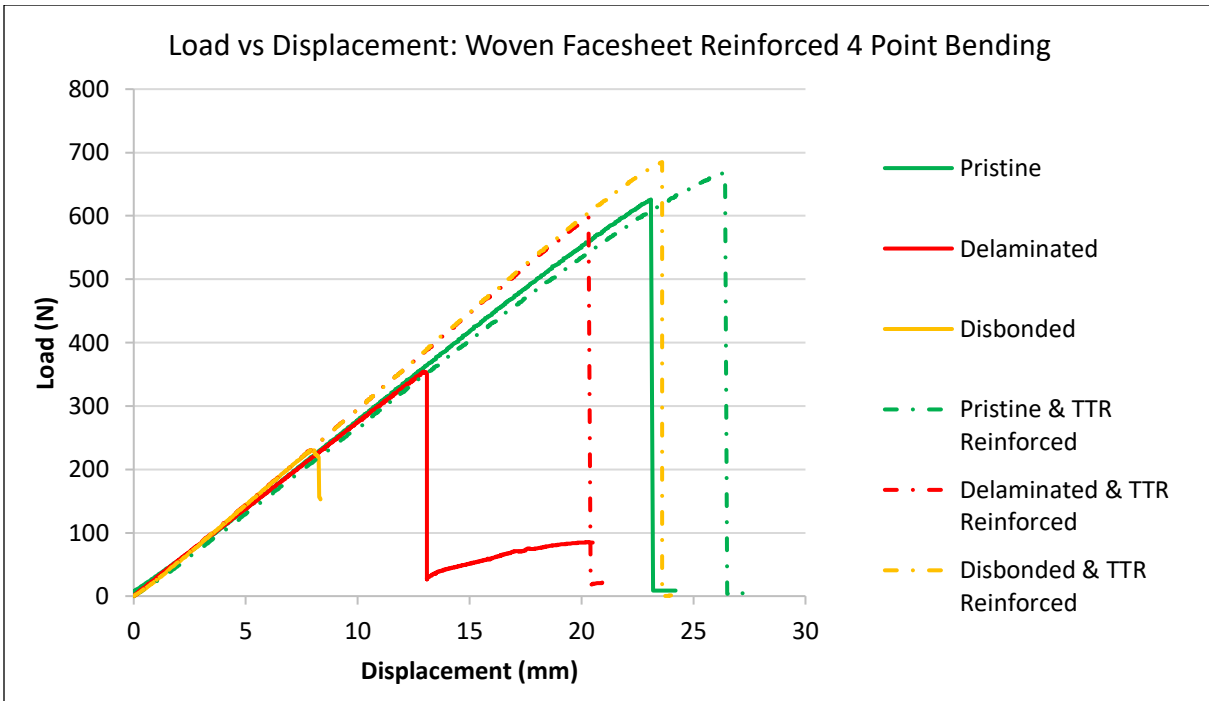
Figure 18: Mr. Suresh's graph comparison of TTR reinforced samples to controls
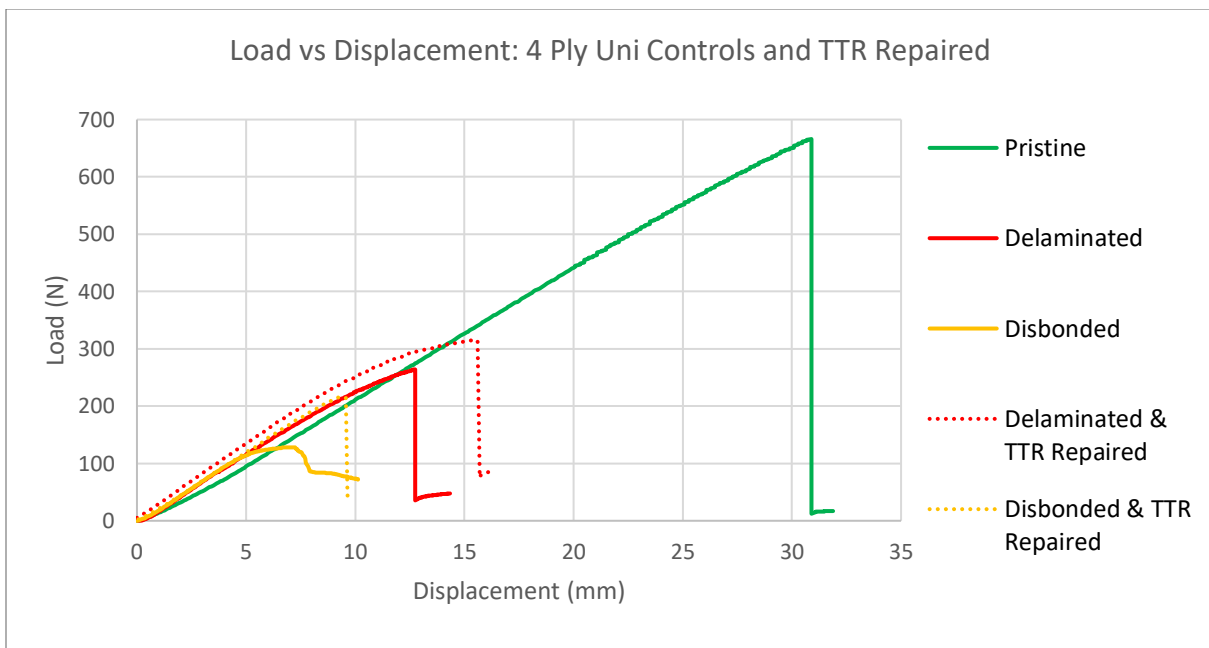
Figure 19: Graph comparison of 4 ply unidirectional TTR repaired samples to controls

Load vs Displacement: 4 Ply Uni Controls and TTR Reinforced
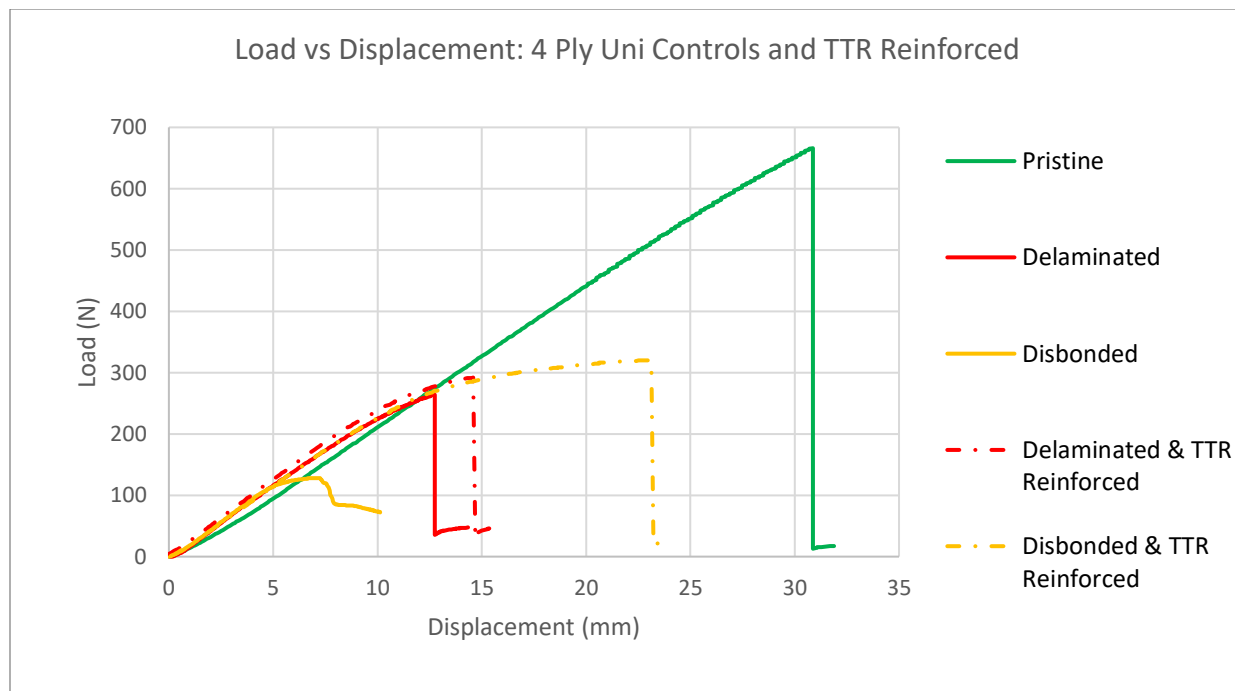
Figure 20: Graph comparison of 4 ply unidirectional TTR reinforced samples to controls

The data in Tables 1, 2, and 3 show an overview of all unidirectional four ply samples, including their failure loads, obtained stiffness values, and failure types. Following these tables, images of these samples during and after failure help to visualize the different failure types.

Table 1: Unidirectional 4 Ply Bending – Pristine Data

Pristine 4-Ply Unidirectional Samples			
Sample	Max Load (N)	Stiffness (N/mm)	Failure Type
4U-PRI-1	671	22.381	Facesheet Failure Under Roller
4U-PRI-2	707	23.353	Facesheet Failure Under Roller
4U-PRI-3	599	22.215	Facesheet Failure Between Rollers
4U-PRI-4	666	23.025	Facesheet Failure Between Rollers
Average	660.75	22.7435	
Standard Deviation	39.002	0.464	
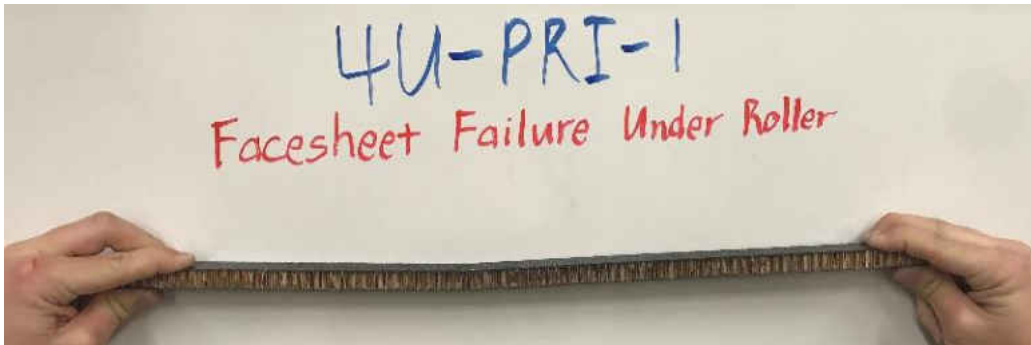
Figure 21: Failure of 4 ply unidirectional pristine sample under roller
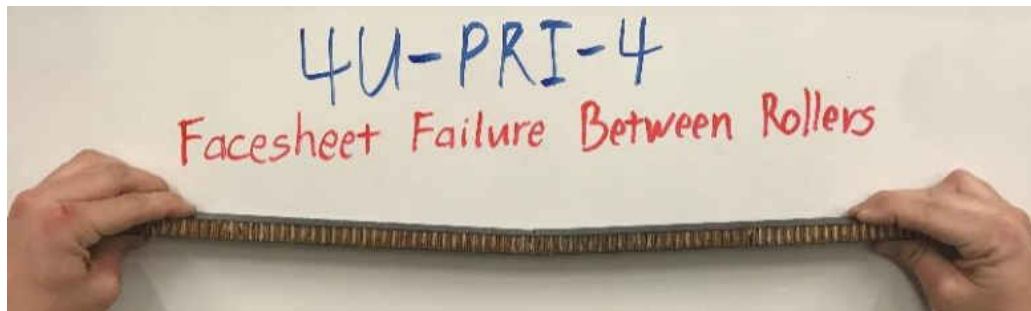
Figure 22: Failure of 4 ply unidirectional pristine sample between rollers

Table 2: Unidirectional 4 Ply Bending – Delaminated Data

Delaminated 4-Ply Unidirectional Samples			
Sample	Max Load (N)	Stiffness (N/mm)	Failure Type
4U-DEL-1	250	23.311	Crack Propagation
4U-DEL-2	266	24.186	Crack Propagation
4U-DEL-3	264	23.857	Crack Propagation
Average	260	23.785	
Standard Deviation	7.12	0.36	

Delaminated 4-Ply Unidirectional Repaired Samples			
Sample	Max Load (N)	Stiffness (N/mm)	Failure Type
4U-DEL-1-TTR_Repaired	289	24.814	Facesheet Failure Between Rollers
4U-DEL-2-TTR_Repaired	316	26.153	Facesheet Failure Between Rollers
4U-DEL-3-TTR_Repaired	324	25.23	Facesheet Failure Between Rollers
Average	309.67	25.40	
Standard Deviation	14.97	0.56	
Percent Effectiveness	19.1%	6.8%	

Delaminated 4-Ply Unidirectional Reinforced Samples			
Sample	Max Load (N)	Stiffness (N/mm)	Failure Type
4U-DEL-4-TTR_Reinforced	292	24.899	Facesheet Failure Between Rollers
4U-DEL-5-TTR_Reinforced	294	25.017	Facesheet Failure Between Rollers
Average	293	24.958	
Standard Deviation	1	0.059	
Percent Effectiveness	12.7%	4.9%	

Figure 23: Failure of 4 ply unidirectional delaminated sample
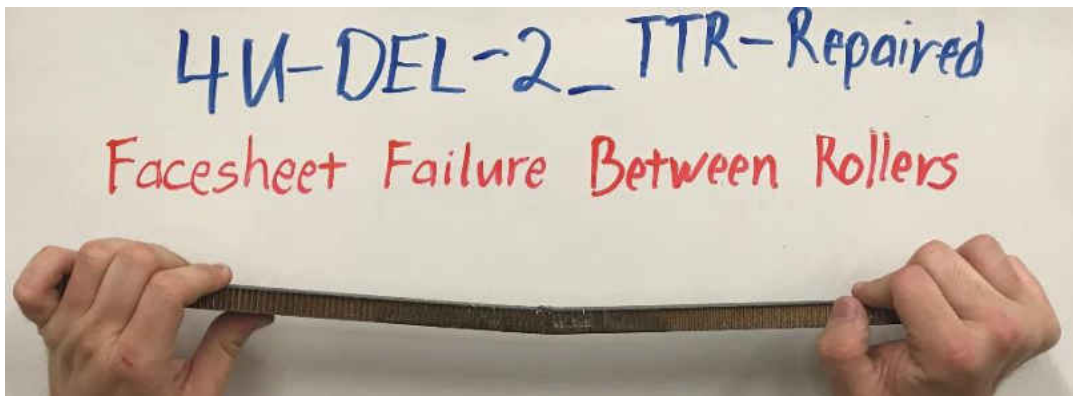
Figure 24: Failure of 4 ply unidirectional delaminated & TTR repaired sample
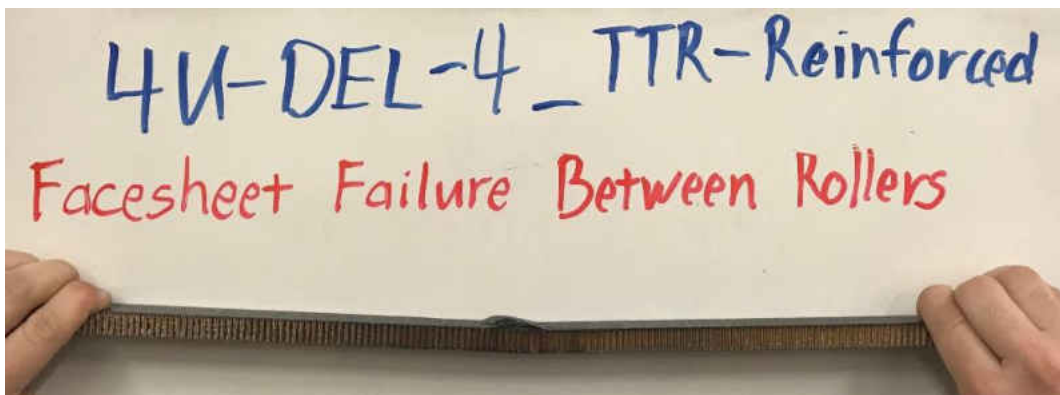
Figure 25: Failure of 4 ply unidirectional delaminated & TTR reinforced sample

Table 3: Unidirectional 4 Ply Bending – Disbonded Data

Disbonded 4-Ply Unidirectional Samples			
Sample	Max Load (N)	Stiffness (N/mm)	Failure Type
4U-DIS-1	129	23.9	Facesheet Failure / Crack Propagation
4U-DIS-2	125	25.732	Facesheet Failure / Crack Propagation
4U-DIS-3	128	25.255	Facesheet Failure / Crack Propagation
Average	127.333	24.962	
Standard Deviation	1.700	0.776	

Disbonded 4-Ply Unidirectional Repaired Samples			
Sample	Max Load (N)	Stiffness (N/mm)	Failure Type
4U-DIS-1-TTR_Repaired	186	23.349	Facesheet Failure Between Rollers
4U-DIS-2-TTR_Repaired	238	24.558	Facesheet Failure Between Rollers
4U-DIS-3-TTR_Repaired	216	24.643	Facesheet Failure Between Rollers
Average	213.33	24.18	
Standard Deviation	21.31	0.59	
Percent Effectiveness	67.5%	-3.1%	

Disbonded 4-Ply Unidirectional Reinforced Samples			
Sample	Max Load (N)	Stiffness (N/mm)	Failure Type
4U-DIS-4-TTR_Reinforced	318	24.412	Facesheet Failure Between Rollers
4U-DIS-5-TTR_Reinforced	320	23.74	Facesheet Failure Between Rollers
Average	319.00	24.08	
Standard Deviation	1.00	0.34	
Percent Effectiveness	150.5%	-3.6%	
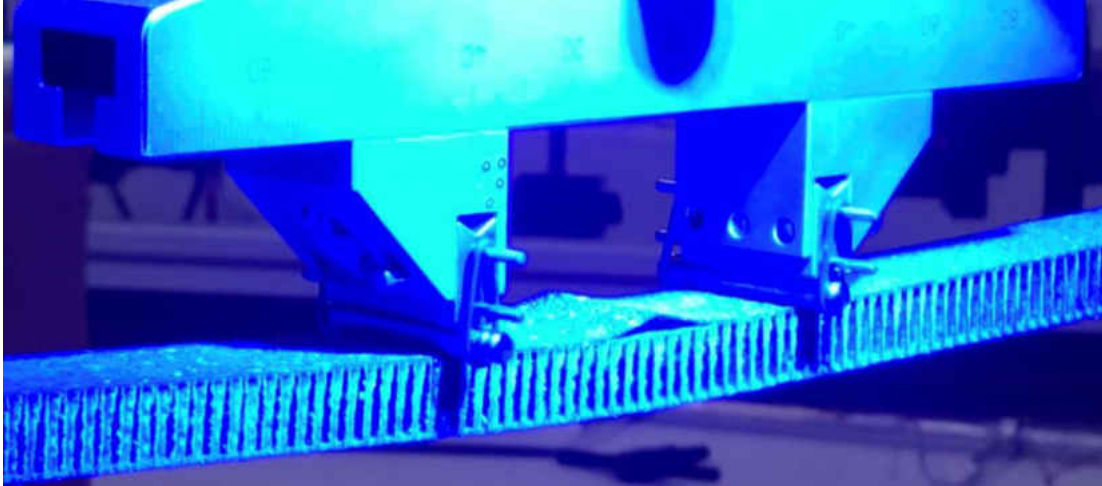
Figure 26: Failure of 4 ply unidirectional disbonded sample

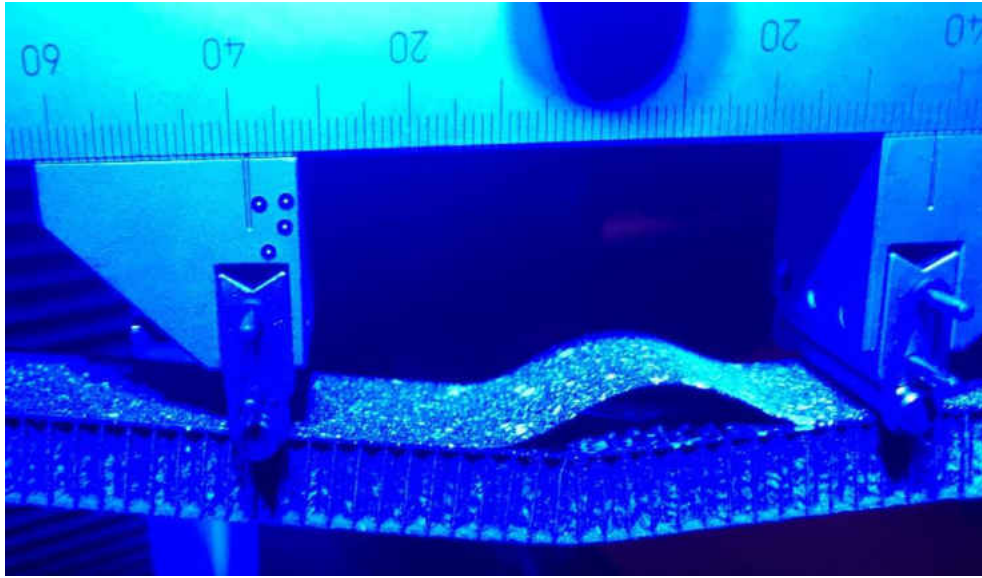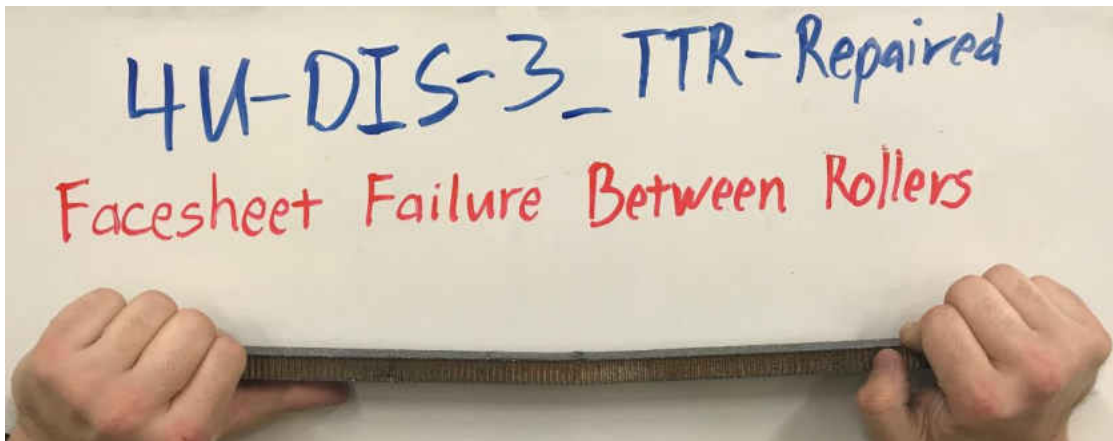Figure 27: Failure of 4 ply unidirectional disbonded & TTR repaired sample
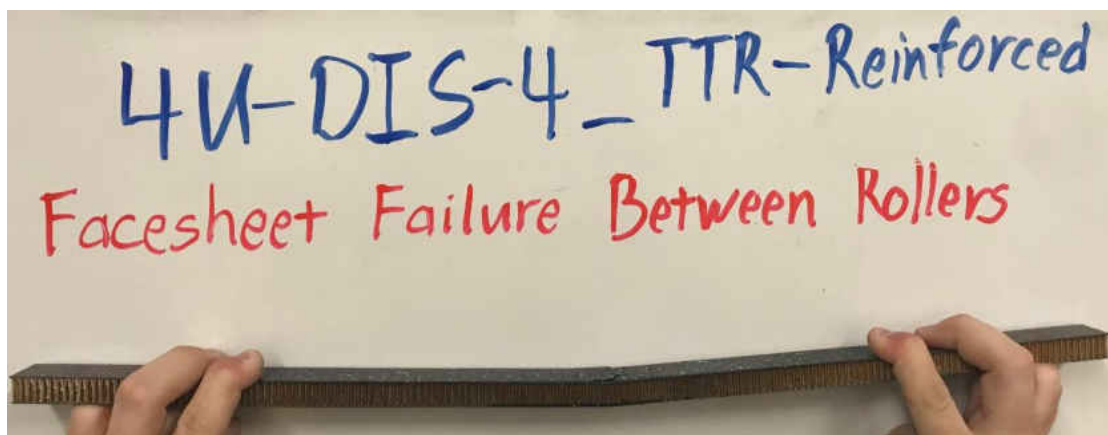
Figure 28: Failure of 4 ply unidirectional disbonded & TTR reinforced sample

While TTR provided a noticeable increase in load carrying capabilities, along with an increase in displacement until failure, this only presents half of the story. In Dr. Kravchenko's study, a test of TTR aspect ratio was conducted, finding a greater aspect ratio improves the effectiveness of the reinforcement or repair. As mentioned in the methods section, an eight ply unidirectional facesheet design was made to test this theory. These samples had a facesheet thickness twice that of the four ply facesheet version and were constructed of the same unidirectional material with the fibers also going lengthwise of the specimens.

Upon testing of the eight ply facesheet samples, a noticeable difference in stiffness and load carrying capacities was observed. Figures 29 through 32 show the loading charts and graphs of the different sample types within the eight ply facesheet design and can be used in comparison to the previously shown charts and figures.
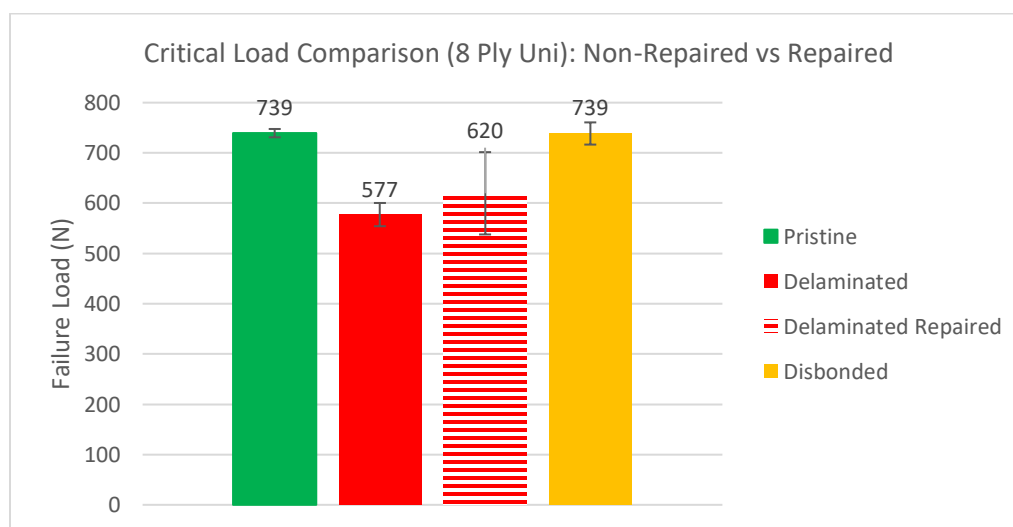
Figure 29: Comparison of unidirectional non-repaired and repaired eight ply samples
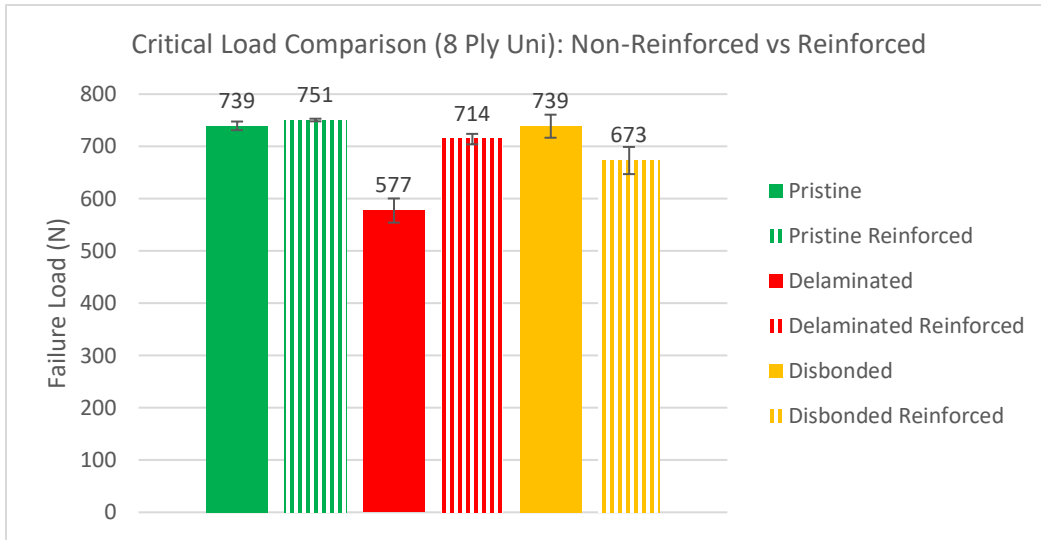
Figure 30: Comparison of unidirectional non-reinforced and reinforced eight ply samples
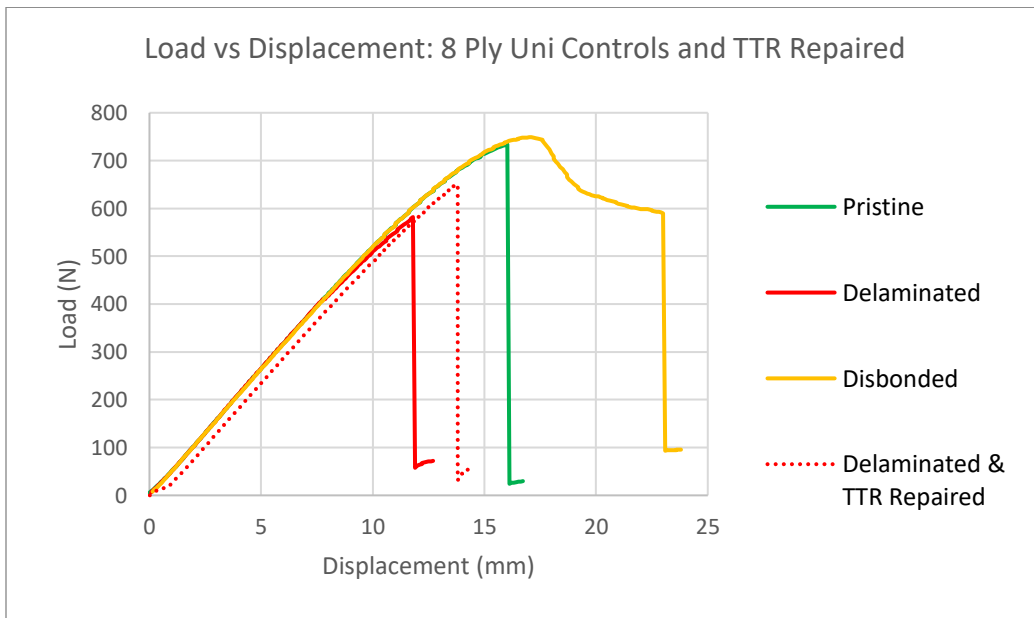
Figure 31: Graph comparison of 8 ply unidirectional TTR repaired samples to controls
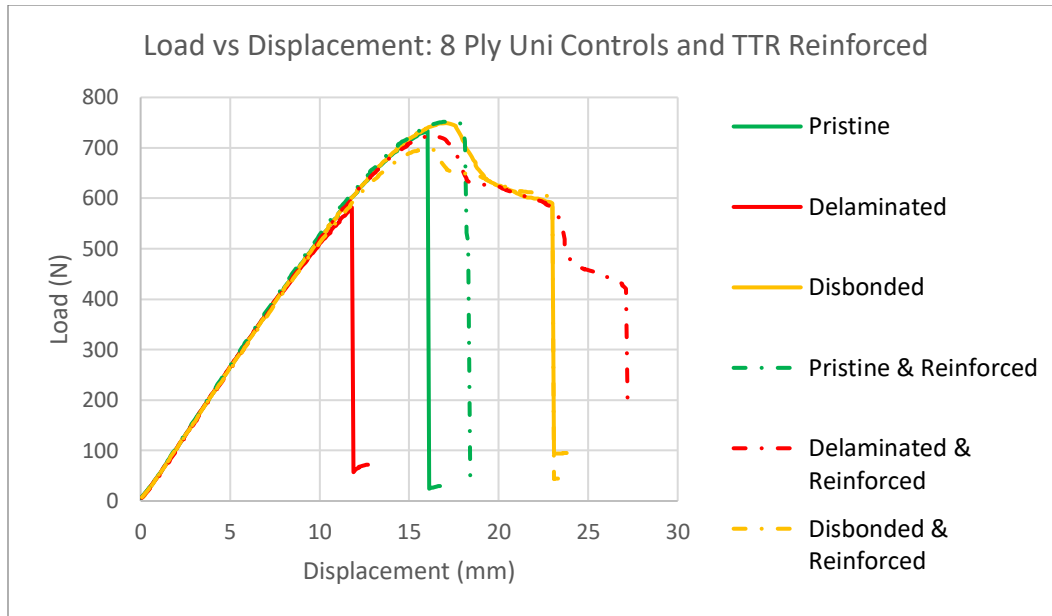
Figure 32: Graph comparison of 8 ply unidirectional TTR reinforced samples to controls

Due to the increase of thickness of the facesheets and the addition of material, higher compressive and tensile loads could occur in the upper and lower facesheets, respectively. Unfortunately, this led to an issue where the limit of the core was approached. While the upper facesheet was undergoing compression, the upper facesheet experienced tension, causing a shearing effect in the core under high loads.   This effect can be visualized in the load vs displacement curves where the slopes go to zero and a peak load is reached.

In Figures 29 and 31, the data for the eight ply facesheet disbonded and repaired TTR samples appears to be missing; however, due to the failure type of the disbonded samples in the core, TTR would not be an effective repair. The shearing of the core occurs outside of the maximum moment region where another type of repair may be more suitable.

In regard to the effectiveness of through thickness reinforcement in the defected eight ply facesheet samples, there were seemingly conflicting results. While the effectiveness for the

delaminated repaired and delaminated reinforced samples had increasing positive values respectively, the disbonded reinforced samples had a negative effectiveness value. Further analysis of this data can be made in the tables and figures below.

Table 4: Unidirectional 8 Ply Bending – Pristine Data

Pristine 8-Ply Unidirectional Samples			
Sample	Failure Load (N)	Stiffness (N/mm)	Failure Type
8U-PRI-1	751	51.569	Shearing of Core
8U-PRI-2	734	51.711	Facesheet Failure
8U-PRI-3	733	52.661	Shearing of Core
Average	739.333	51.980	
Standard Deviation	8.260	0.485	

Pristine 8-Ply Unidirectional Reinforced Samples			
Sample	Failure Load (N)	Stiffness (N/mm)	Failure Type
8U-PRI-4_TTR-Reinforced	753	52.541	Shearing of Core
8U-PRI-5_TTR-Reinforced	748	52.672	Shearing of Core
Average	750.5	52.607	
Standard Deviation	2.5	0.066	
Percent Effectiveness	1.5%	1.2%	
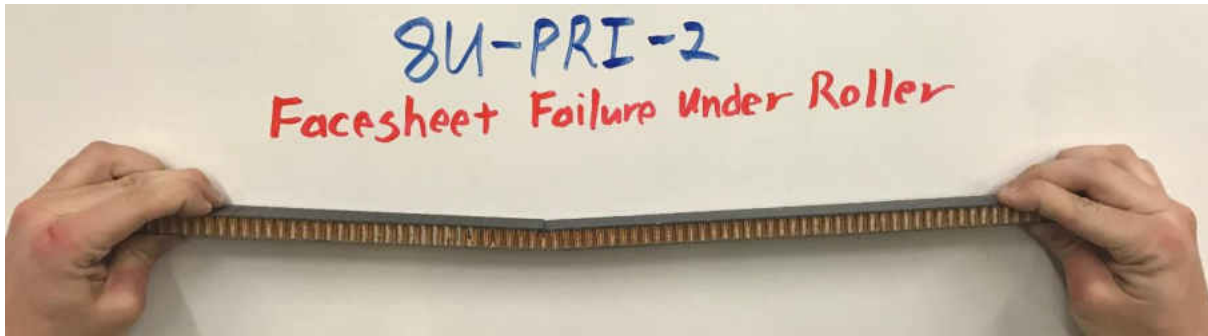
Figure 33: Failure of 8 ply unidirectional pristine sample – facesheet failure
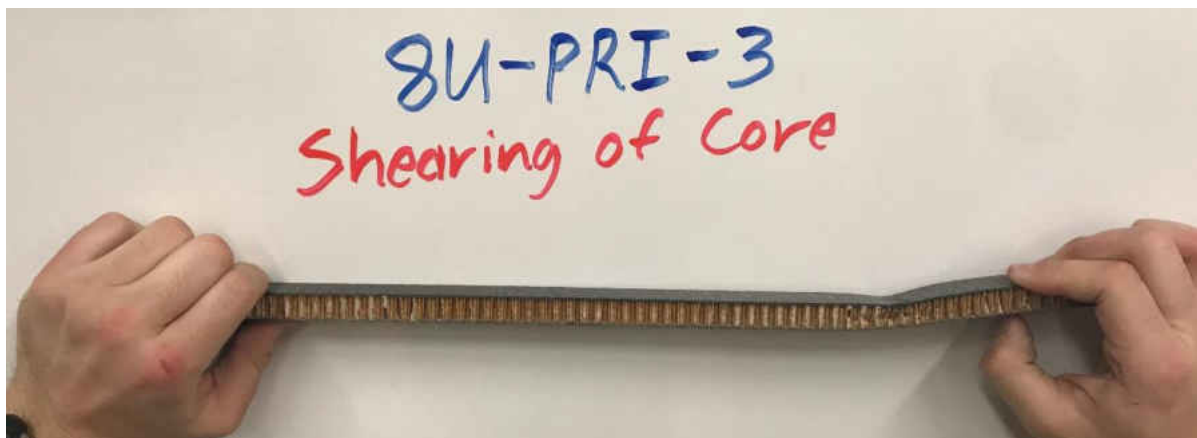
Figure 34: Failure of 8 ply unidirectional pristine sample – core failure
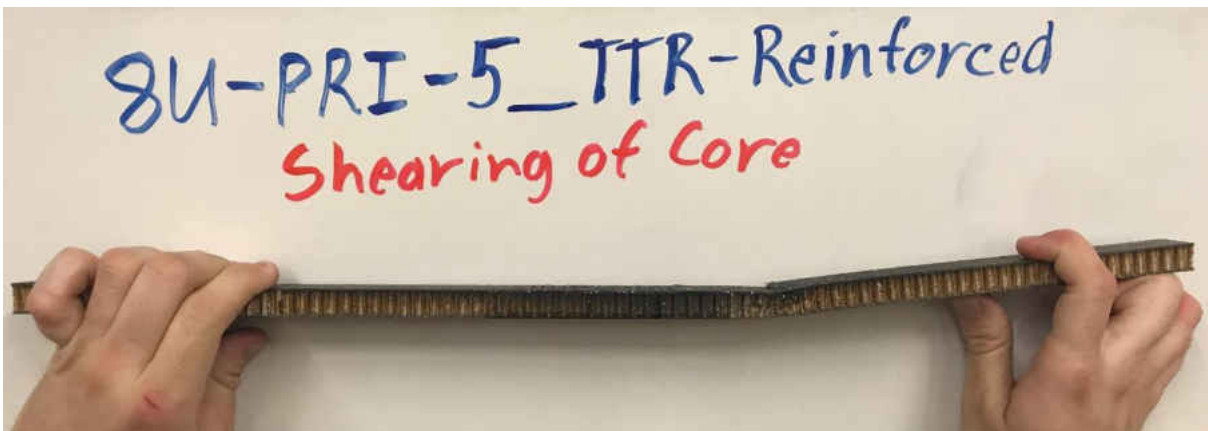
Figure 35: Failure of 8 ply unidirectional pristine TTR reinforced sample

Table 5: Unidirectional 8 Ply Bending – Delaminated Data

Delaminated 8-Ply Unidirectional Samples			
Sample	Failure Load (N)	Stiffness (N/mm)	Failure Type
8U-DEL-1	603	51.149	Crack Propagation
8U-DEL-2	582	51.013	Crack Propagation
8U-DEL-3	547	49.581	Crack Propagation
Average	577.333	50.581	
Standard Deviation	23.099	0.709	

Delaminated 8-Ply Unidirectional Repaired Samples			
Sample	Failure Load (N)	Stiffness (N/mm)	Failure Type
8U-DEL-1_TTR-Repaired	702	50.892	Shearing of Core
8U-DEL-2_TTR-Repaired	649	50.953	Facesheet Failure Under Roller
8U-DEL-3_TTR-Repaired	508	49.531	Facesheet Failure Between Rollers
Average	619.667	50.459	
Standard Deviation	81.871	0.656	
Percent Effectiveness	7.3%	-0.2%	

Delaminated 8-Ply Unidirectional Reinforced Samples			
Sample	Failure Load (N)	Stiffness (N/mm)	Failure Type
8U-DEL-4_TTR-Reinforced	704	50.616	Facesheet Failure Between Rollers
8U-DEL-5_TTR-Reinforced	724	52.345	Shearing of Core
Average	714	51.481	
Standard Deviation	10	0.865	
Percent Effectiveness	23.7%	1.8%	

Figure 36: Failure of 8 ply unidirectional delaminated sample

Figure 37: Failure of 8 ply unidirectional delaminated TTR repaired sample (1)

Figure 38: Failure of 8 ply unidirectional delaminated TTR repaired sample (2)
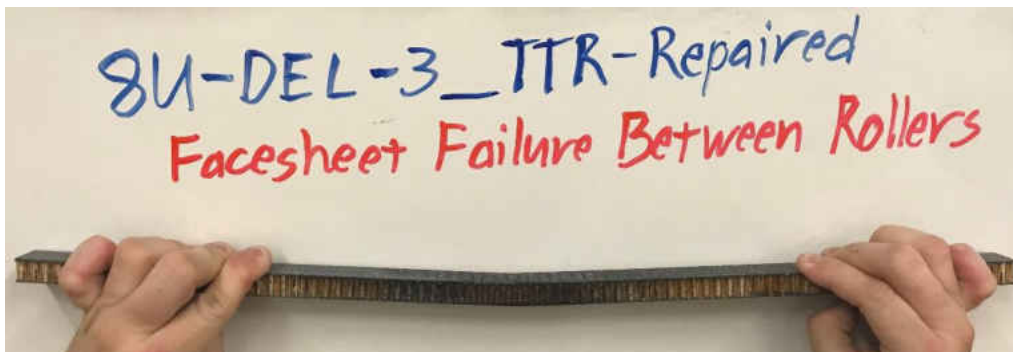
Figure 39: Failure of 8 ply unidirectional delaminated TTR repaired sample (3)
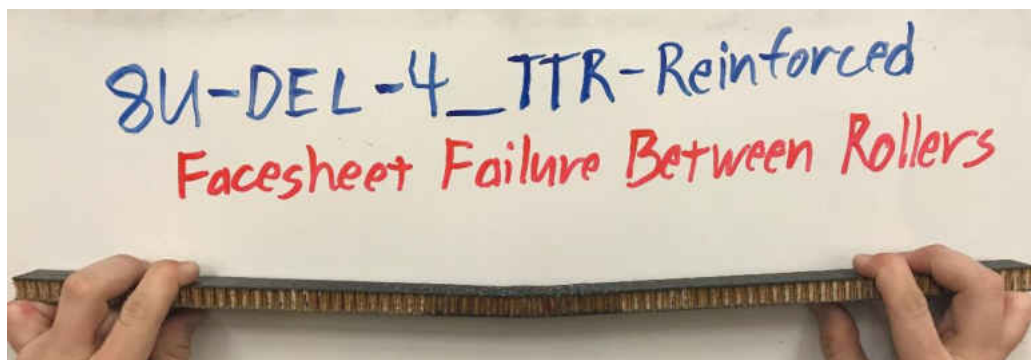
Figure 40: Failure of 8 ply unidirectional delaminated TTR reinforced sample (1)
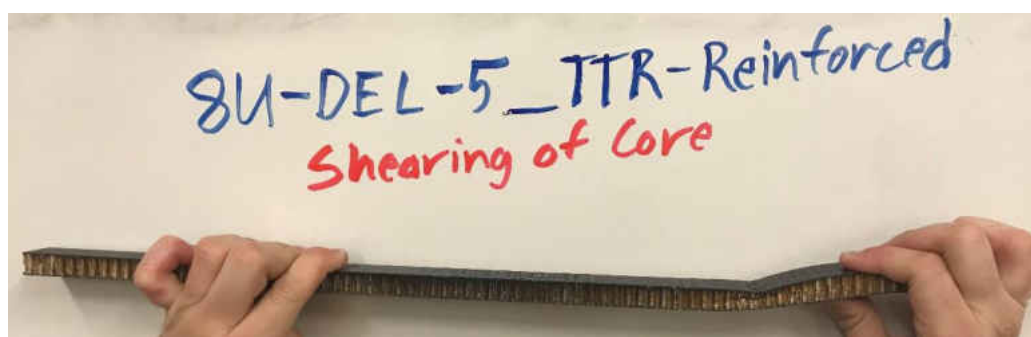
Figure 41: Failure of 8 ply unidirectional delaminated TTR reinforced sample (2)

Table 6: Unidirectional 8 Ply Bending – Disbonded Data

Disbonded Samples			
Sample	Failure Load (N)	Stiffness (N/mm)	Failure Type
8U-DIS-1	708	51.028	Shearing of Core
8U-DIS-2	759	52.407	Shearing of Core
8U-DIS-3	749	51.762	Shearing of Core
Average	738.667	51.732	
Standard Deviation	22.066	0.563	

| Disbonded Reinforced Samples			
Sample	Failure Load (N)	Stiffness (N/mm)	Failure Type
8U-DIS-4_TTR-Reinforced	647	50.74	Facesheet Failure Between Rollers
8U-DIS-5_TTR-Reinforced	699	50.646	Shear Core Failure
Average	673	50.693	
Standard Deviation	26	0.047	
Percent Effectiveness	-8.9%	-2.0%	
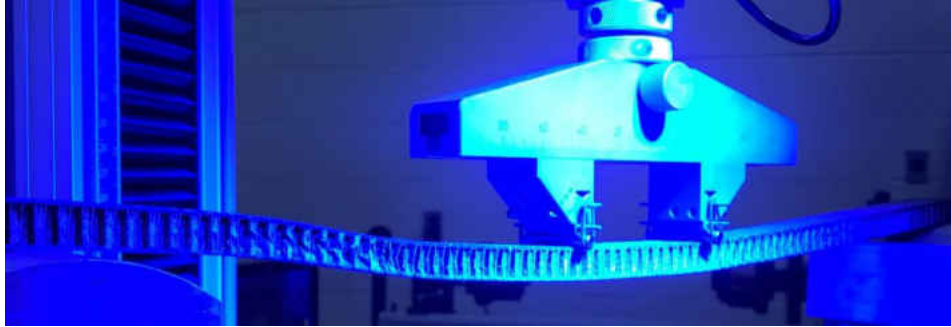
Figure 42: Failure of 8 ply unidirectional disbonded sample

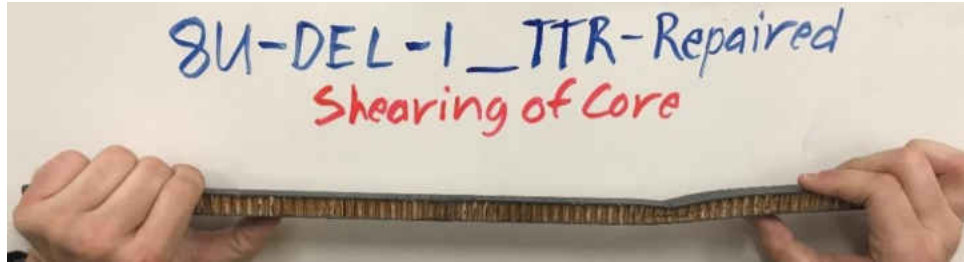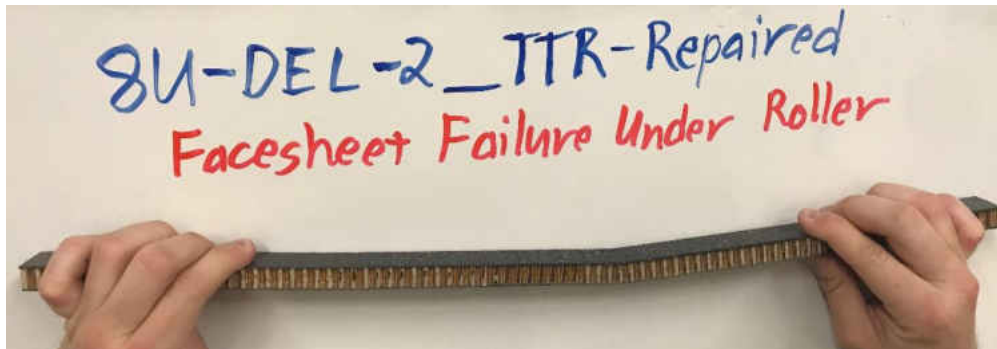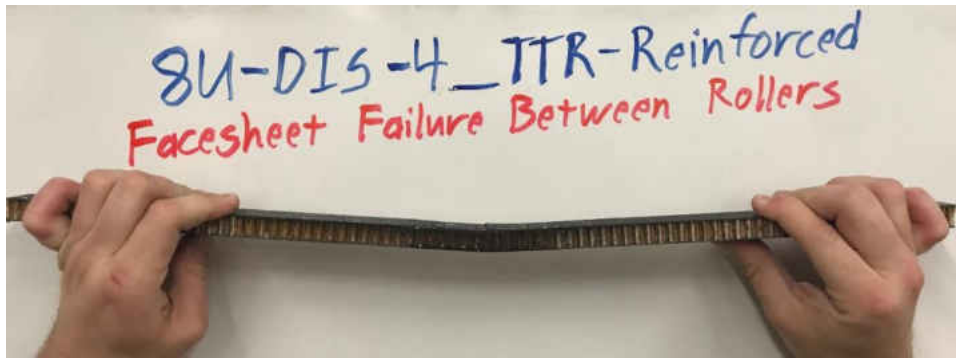*Figure 43: Failure of 8 ply unidirectional disbonded TTR reinforced sample (1)*
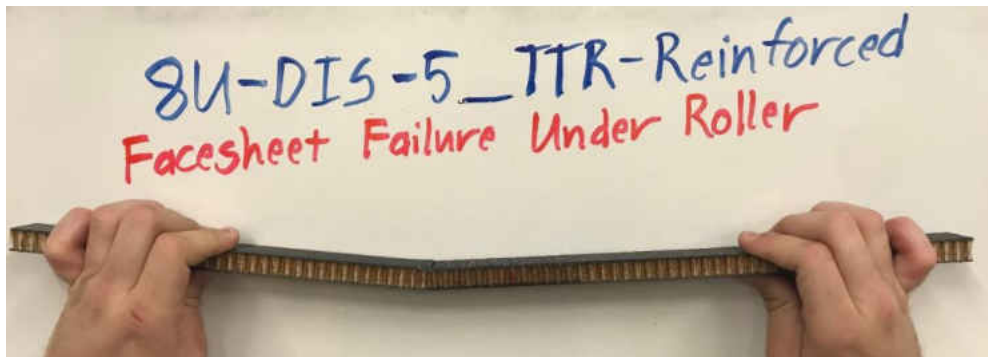
Figure 44: Failure of 8 ply unidirectional disbonded TTR reinforced sample (2)

FOUR-POINT BENDING DISCUSSION

As this study was a continuation of Mr. Suresh's research, many of the same characteristics from his experimentation were found here. From the knockdown effects of the delaminated and disbonded samples to the improvement in load carrying capacity in the TTR repaired and reinforced samples, the trends were for the most part expected from prior experimentation.

This study was not only to further the four-point bending data from Mr. Suresh but to also investigate the concept of aspect ratio from Dr. Kravchenko's studies on this design. As expected, a facesheet with more plies holds more load. The unexpected result was in the shearing of the core. The three pound density Nomex honeycomb was unable to handle the higher compressive and tensile loads between the upper and lower facesheets and became the weak point for many samples.

One portion of the eight ply facesheet study that showed promising results was in the delaminated data. While the pristine and disbonded samples proved to be a too-strong design and failed the core prior to the facesheet, the weak point of the delaminated samples was the facesheet in all configurations. This allowed for an accurate investigation of the effectiveness of TTR. Further investigation with a different core thickness and density would be necessary to gain back the data of the pristine and disbonded samples, as a study performed in 2018 looked into maximizing the three-point bend loading of aluminum core composites for automobile manufacturing.[21] Core supports could also be an option in order to keep the same sample geometry and material.[22]

When comparing the effectiveness of TTR between the four ply and eight ply configurations of delaminated samples, the repair effectiveness values were 19.1% and 7.3%, respectively. While this may almost disprove the aspect ratio theory, a low sample size was obtained, and the third delaminated eight ply sample had a much lower than average failure load than the other two samples like it. Moving on to the effectiveness of TTR as a reinforcement method, the effectiveness values were 12.7% and 23.7% for the four ply and eight ply configurations, respectively. Unlike the repaired and delaminated samples, both delaminated and reinforced data sets had small standard deviation values, providing a greater confidence in the obtained percentages.

Not only did the TTR in the eight ply configuration prove itself by increasing failure load and effectiveness in reinforcement, but it also had to overcome the problem of increased crack propagation. The images below are taken from the DIC and help to show the failure of the four and eight ply delaminated samples. While a good surface was obtained for the four ply facesheet samples, there were difficulties with lighting for the eight ply facesheet samples; however, crack propagation can be clearly identified.
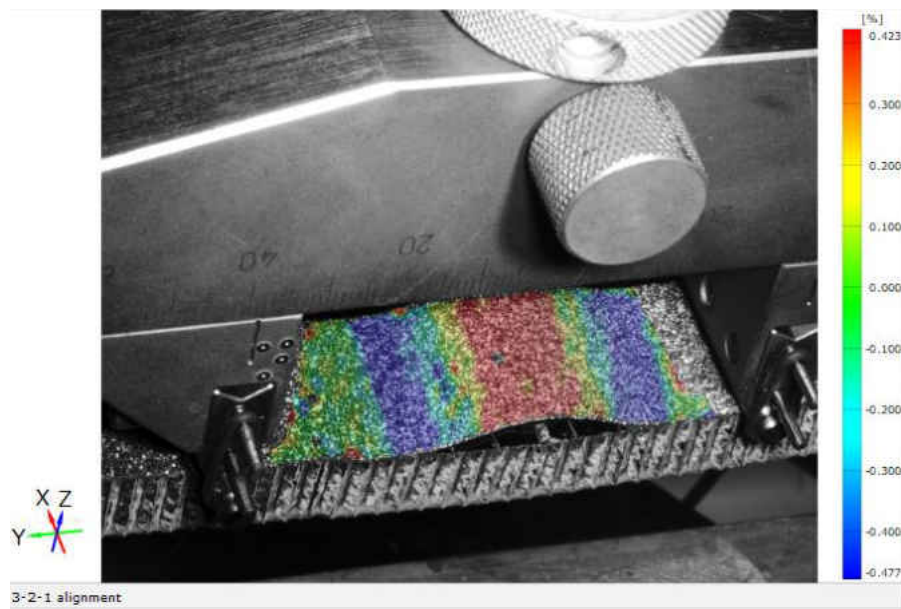
Figure 45: DIC image of delaminated 4-ply unidirectional sample at failure
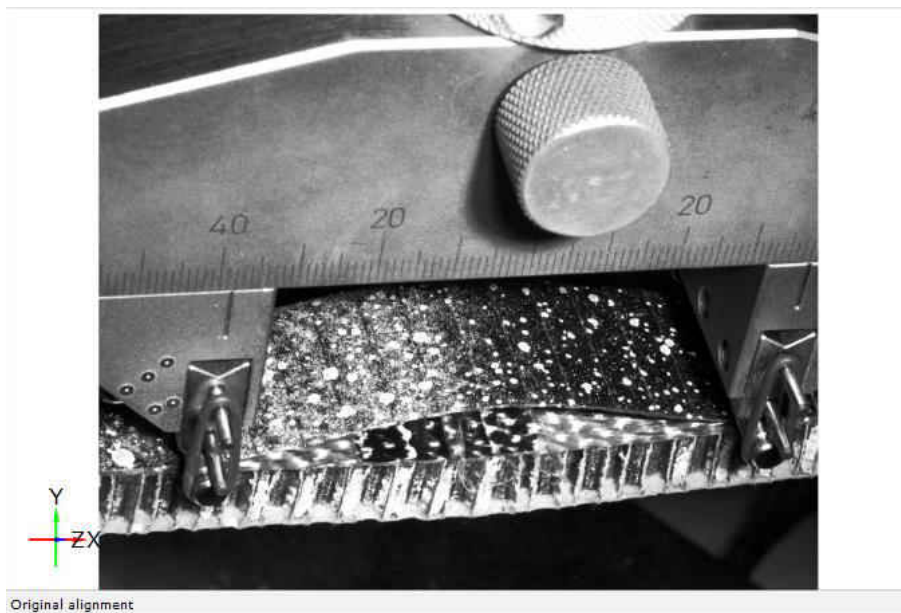
Figure 46: DIC image of delaminated 8-ply unidirectional sample at failure

Once the failures in the above images were observed, the samples were unloaded and TTR was applied in the form of repair. The goal of TTR in the four ply facesheet samples with the delamination was to allow for a higher load to be obtained while preventing further propagation

of the crack. In the eight ply facesheet samples with the delamination, the TTR repair was to keep the crack closed and the fibers aligned in the facesheet, given the crack couldn't propagate beyond the rollers.

Figures 47 and 48 show DIC images of visualized strain for the TTR repaired delaminated samples of the four ply and eight ply facesheet configurations, respectively. Both samples were resprayed for DIC image clarity following the TTR process. During testing of the eight ply facesheet samples with the delamination and TTR repair, the samples start with a full strain visualized surface which shrinks in size as the top surface of the sample moves outside of the region where the DIC can pick up the surface.
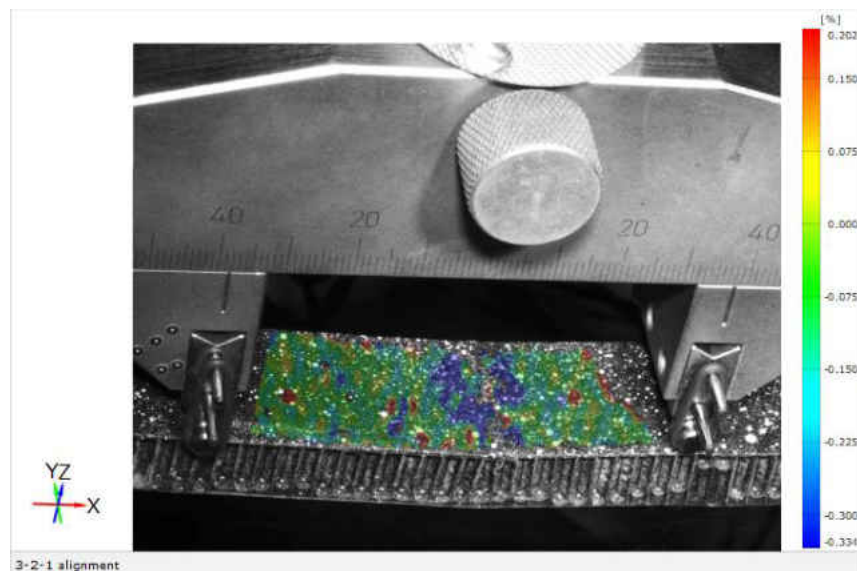
Figure 47: DIC image of delaminated 4-ply unidirectional sample with TTR repair at failure
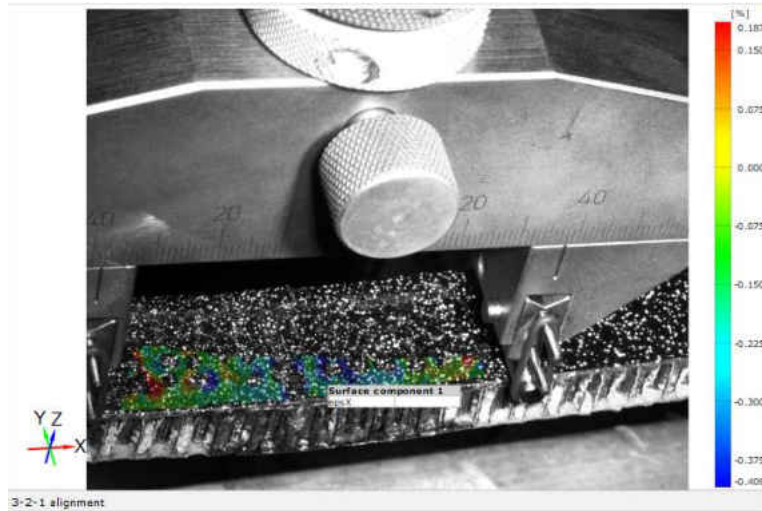
Figure 48: DIC image of delaminated 8-ply unidirectional sample with TTR repair at failure

While the carbon rods in the TTR repair cannot be easily seen in the DIC imaged, the locations of the rods become apparent as localized spots of lower stress show up and begin to form a "band" of stress across the width of the facesheet surface prior to failure of the sample. Figure 49 helps to show this phenomenon the instant before failure of the same sample as shown in Figure 47.
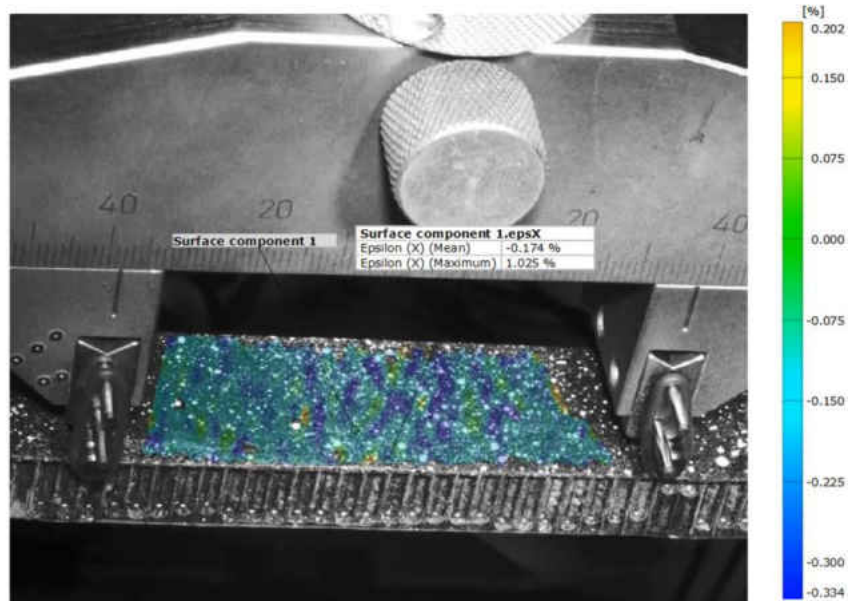
Figure 49: DIC image of sample with TTR repair prior to failure

Additional work may be required to further prove the increase in TTR effectiveness in four-point bending as a function of facesheet thickness; however, a noticeable trend in this data was obtained. Future experimentation in this specific problem may be worthwhile with a higher density core that is more resilient to shear forces, as 6 lb and 9 lb densities are available from Rock West Composites.[23] An increase in the number of samples would be beneficial as well, as a quicker and more effective fabrication method would ideally be used (and will be discussed towards the end of the next section).

DOUBLE LAP JOINT METHODOLOGY

As was introduced in the background section, the joining of composites has become an area of interest in the engineering world, specifically with large honeycomb composite structures. To further explore this area and to see where possible improvement could take place, experimentation of through thickness reinforcement to this type of joint seemed like a worthwhile investigation.

The investigation of applying TTR to adhesively bonded joints begins at the sample design. NASA's test specimens are cured as one big carbon fiber honeycomb plate in an autoclave and measure 3" wide by 22" long when cut. The core used for their samples was a 1" thick aluminum honeycomb material and had to be milled out of each end of every sample for a machined aluminum adaptor to be cured into the structure for tension testing. (Figures 50 and 51)
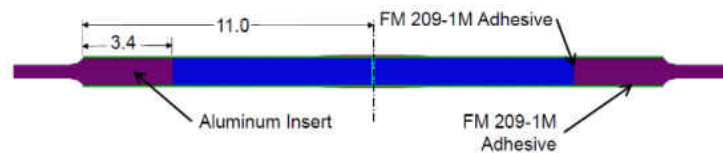
Figure 50: NASA's double lap joint sample design
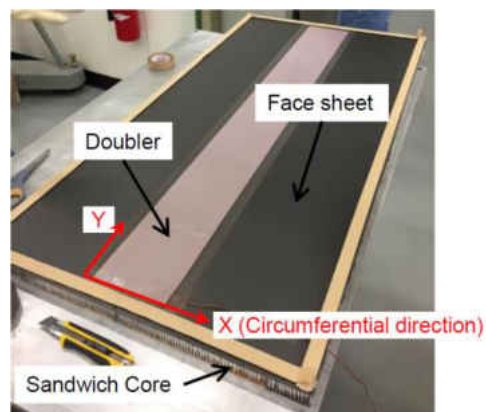
Figure 51: NASA's manufacturing of a panel

To best maximize time, materials, and available tools, a variation of this design was proposed. The new dimensions of the composite structure would be 2.5" by 18" to allow for proper fitment on the 12" by 24" aluminum plate tool lengthwise. Another reason for these revised dimensions was for the co-curing of the end adaptors during the curing of the honeycomb composite structure, adding another 1.5" on each end of the plate. This method could save time, and there would be fewer concerns in regard to possible alignment issues. The reduction in width was made in an effort to maintain a similar length to width ratio as NASA's samples and to have a constant far field stress across the width of the sample in the location of the joint. A Solidworks CAD model was made to visualize the sample to be made (Figure 52).
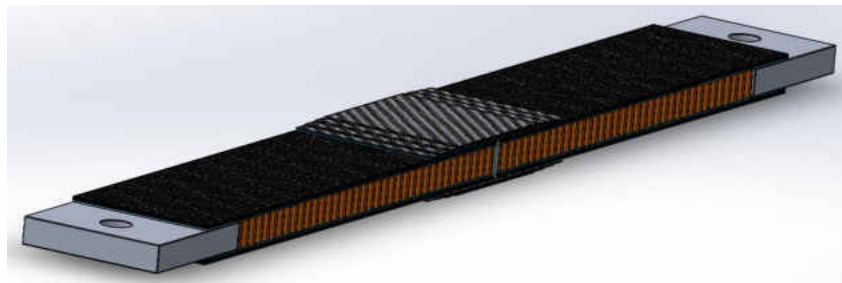
Figure 52: Solidworks model of sample design for this experiment

As for materials, a Nomex honeycomb core of 0.460" was chosen, as it was in stock from the previous experiment discussed. The same Fibreglast unidirectional carbon fiber prepreg was used from the four-point bending samples for the same reason. While NASA used an eight ply quasi-isotropic $[45/90/-45/0]_s$ layup for their facesheets, a simple $[0]_6$ layup was chosen. This facesheet design would allow for high stiffness and strength while decreasing fracture toughness, which would allow for crack propagation to occur and would put TTR to the test. For the

adhesively bonded joint, Fibreglast's carbon fiber woven prepreg was used with the direction of the fibers going length-wise and width-wise, as opposed to NASA's [45]$_4$ layup. The chosen orientations for the facesheets and the joints helped to reduce material waste and to simplify the fabrication process.

Since all facesheet plies were to be unidirectional and the joint area was oriented in a 0˚ manner, a very high load and stiffness was expected. In response, an end adaptor made of 4140 steel, rather than aluminum, was chosen. This would help increase critical load of the sample (should it approach the limits of the selected end adaptor material), decrease deflection within the end adaptor, and reduce material cost. Due to the size of our chosen aluminum plate tool, it was only feasible to manufacture a plate that could only make two samples at a time. An end adaptor was designed that would allow for at least two samples to be made from it, have a pinned connection, and have at least 1" by 2.5" of adhesive bond. The ODU machine shop machined these adaptors (Figures 53 and 54).
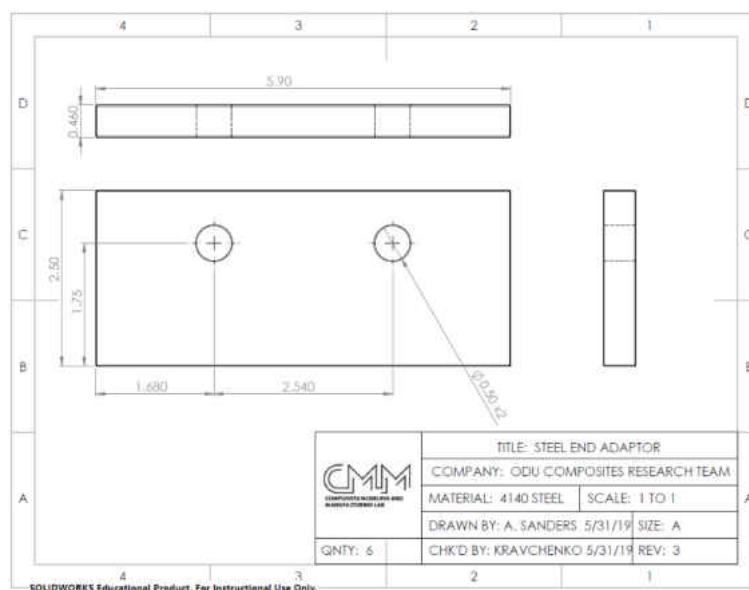
Figure 53: CAD drawing of end adaptor plate

Figure 54: Machining of end adaptor plate in ODU's machine shop

For construction of the plates, a traditional layup method was used, as a full plate without a gap or joint was initially made. As mentioned before, the facesheets on each side were six plies, all with a 0˚ orientation. Just as in the four-point bending samples, the same 0.460" thick Nomex honeycomb material was used for the core, as was the Loctite EA 9696 adhesive film. An added element to the layup was the insertion of the steel end adaptors. Careful consideration of the alignment of the steel end adaptors was taken. Figure 55 shows the basic layup procedure with separate plies of carbon fiber prepreg laid underneath the adaptors with a teflon layer between to prevent curing to the adaptors.

Figure 55: Fabrication of a double lap joint panel

Three different types of panels were manufactured: pristine, 0.25" teflon defect, and 0.5" teflon defect. The pristine sample had a six ply facesheet with no manufactured defects, which was the simplest layup of all the samples. The 0.25" defected panels had a half inch wide strip of teflon between the fifth and sixth plies outward from the core that was laid across the width of the panel, centered length-wise. The 0.5" defected panels would use the same principal but with an inch wide teflon strip instead. The question that arose with these defects was if this would lead to an increase or decrease in ultimate load. On one hand, you have a crack of bigger and bigger magnitude that is susceptible to growth, leading to a failure before that of a pristine sample. On the other hand, there could be a question regarding compliance in the joint region possibly helping to hold the crack propagation off until a higher load is achieved. Another question that arises is the effectiveness in through thickness reinforcement in this scenario and if it would help to increase the peak loading of samples, prevent crack propagation, or neither.

Once the plate was laid up and the vacuum bag was sealed, the process then moved to the heat press, where the sample was cured at 80˚C and 20psi for two hours, then 130˚C and 80psi for four hours, all under vacuum. The plate was then cut in half width-wise in the OMAX ProtoMAX waterjet machine. After drying and cleaning of the cut plate pieces, a 0.1" gap was set and filled with Lord 310 A/B epoxy (Figure 56). Once the epoxy in the gap was cured, any excess was scraped or sanded off. Then the bonding surface was prepared with sandpaper and acetone for the addition of the adhesive film and carbon fiber woven prepreg plies for the joining of the plate pieces.[24] Just as in NASA's design, the layers of carbon fiber were cut to the width of the plate and stacked in the following lengths: 3.0", 2.4", 3.6", and 4.2" (Figure 57).
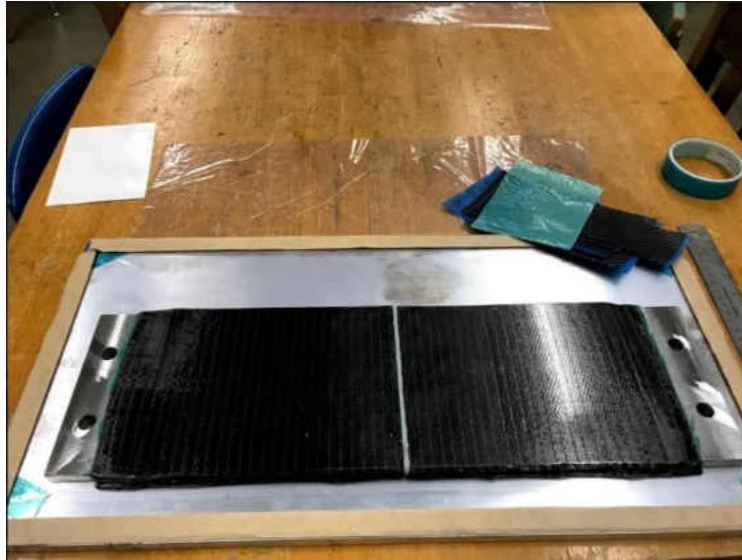
Figure 56: Cut panel with epoxy filled gap
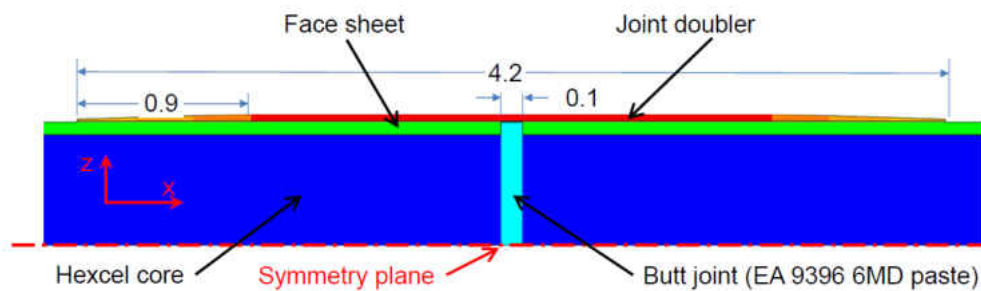
Figure 57: NASA's doubler joint layup procedure

For the lap joints, layup and curing was performed one side at a time, as a flat surface is ideal when pressure is applied. Curing of the joints retained the same temperature settings and time intervals in the heat press; however, no hydraulic pressure was applied to the joint. This was to prevent the crushing of the core and weakening of the facesheet. When it came to flipping the plate over and curing the joint on the other side, a layered cardboard bed was used to help keep the top of the sample flat, given the bottom side of the plate in this cure cycle was not flat as it had the first joint cured to it. The main concern in this step was that under vacuum, the

pressure alone without the cardboard bed would crack the epoxy filled gap open, causing a misalignment at the joint.

Once the joints are cured, the plate has a second round of cutting in the waterjet machine (Figure 58). A line is carefully drawn up the center of the plate length-wise, where the plate is cut up the center and +/- 2.540" offset from that center line. Due to the non-uniformity of the materials in the plate, a shorter 2.75" cutting path was made to cut through the steel end section while a quicker 12" cutting path did the rest of the cutting past the center of the plate. Just like the four-point bending samples, the plate was longer than 12", which required the plate to be flipped around, lined up, and cut from the other side.

Figure 58: Cutting of double lap joint panel with waterjet machine

Once the samples were cut, they were then dried in an oven at 110˚C and cleaned of cutting abrasive. The samples were then painted for the DIC and tested in tension on an MTS tension / compression testing machine (Figure 59). During testing, both samples were loaded to

8,000 lbf, where the steel end adaptor pulled out of the samples. Under further analysis, it was

found that the steel end adaptor section of the plate when being cured under pressure was not

as forgiving or reluctant to compress as the honeycomb section was, which allowed the adhesive

to squeeze out from between the facesheets and the end adaptors. While the average pressure

across the entire plate may be 80psi, the actual pressure at the steel ends could be much higher.

This realization meant that a uniform displacement method of curing (heat press) would not work

for a composite structure with a nonuniform core. This brings us to a common, more expensive

piece of equipment found in the composites industry, the autoclave.
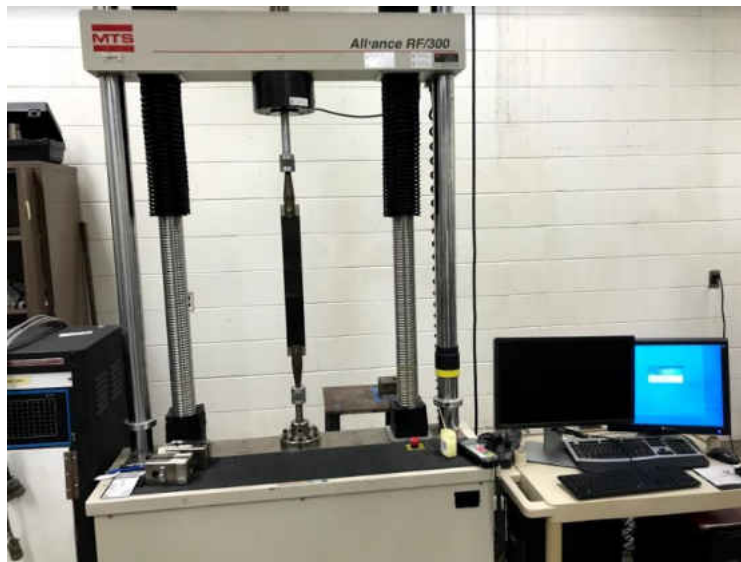
Figure 59: Testing setup for double lap joint samples

Up until this point, the refurbished autoclave had been delivered to Kaufman 128, and

electricity had been run to it, but air and water had not been supplied to the machine, and the

pressure vessel door had not yet been opened. In order to make this project successful, the

autoclave had to be up and running. A few days to get familiar with the machine, its

documentation, and the operation of machines similar to it were required. Then, hoses, fittings, and other items were ordered. Figure 60 shows a schematic diagram that was drawn to display the required hoses and fittings.
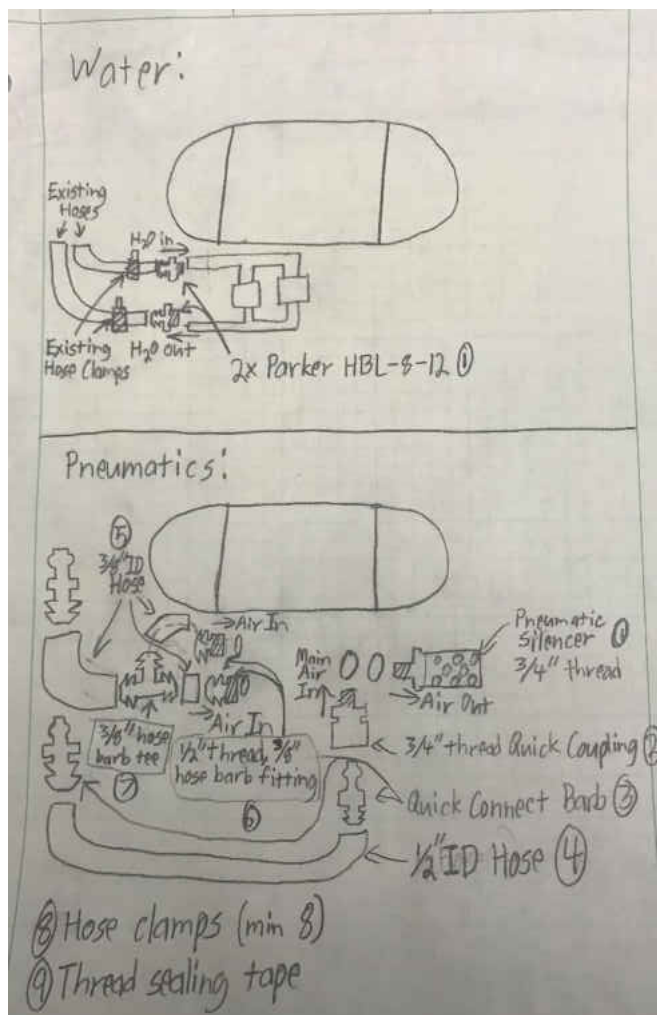
Figure 60: Schematic diagram of air and water sources for autoclave

Once the parts came in and were installed, testing of the autoclave could be conducted. Two of the three phase wires were then swapped, and the autoclave was up and running. Another panel of the same manner as before was manufactured with the same temperature and

pressure parameters, which were programmed to the curing cycle. Unfortunately, this panel did not turn out so well, due to a lack of autoclave fabrication experience (Figure 61). This led to research of the caving in problem, where a solution in tapering was brought to my attention. From a study performed by the Hexcel Corporation, a tapered angle of 30 degrees or less to the tool side was found to be ideal and to prevent caving in of the composite panel. [25] Some disadvantages of this tapering method include the amount of material waste, the time and tooling required to make the tapered cuts, and the amount of space that would be taken up on the 12" by 24" tool plate. There was simply not going to be enough room for a sample with a tapered core. This theory was tested with a core cut by hand (it wasn't pretty), and it was clear that another solution had to be devised (Figure 62).

Figure 61: First fabrication attempt with autoclave

Figure 62: Tapered cutting attempt of honeycomb core

In an effort to reduce or eliminate the caving in of the honeycomb core at its width, a 0.5"
by 0.5" tube stock of steel would be cured in at the sides of the panel. These tubes would help
to support the sides, acting as a tool that becomes a part of the composite structure (Figure 63).
This method proved successful by saving time, money, space, and this project as a whole. Figure
64 shows the results of this method, where a slight bow in the tubing (or small caving in)
occurred; however, this still leaves the structure very rectangular in shape and allows for the
center 5.04" to be used in this experiment.

Figure 63: Panel with steel side supports

Figure 64: Successful curing of a panel in the autoclave

Over the next few weeks, many panels were manufactured until the autoclave
experienced a short in its heating element. At this point, only half of the necessary samples had
been made. The initial sign of this problem was when a fuse for the heating side of the controller
blew. With limited support from the manufacturer due to the out of warranty status of the
machine, a local electrician from Volt Electrical Service was hired and was helpful in identifying

what could be the root cause of the issue. A wire had come loose from one of the top four posts on the heating element and had welded itself to the top of the element, creating a short circuit (Figure 65). A new fuse was ordered, along with new high temperature 8 gauge wire. What would seem like a simple wire replacement would soon become more complicated.

Figure 65: Wiring issue with autoclave

Once the necessary parts were taken out of the autoclave in order to access the heating element, another access problem became apparent. The inside diameter of this machine is approximately 18.25", and the heating element is rectangular on all sides with a front face diagonal dimension very close to this 18.25". This makes it very difficult to put a hand in, much less turn a wrench, as the heating element could not be easily moved out due to its connection to the water pipes, which had fittings on the other side of an insulated aluminum wall.

After many hours of frustration with wrenches and being waist deep horizontal in the pressure vessel, cutting through the insulated aluminum wall became an appealing option. As it would not be a good idea to modify the length of the pipes by cutting them before the fittings,

the solution to cut through the wall around the pipe with a hole saw, although a very brute approach, was determined to be the best solution. A repair for the hole being made was thought out well in advance of the first cut, as it was important to also improve the machine's future serviceability. As the insulated wall was very thick, a special tool had to be made in order to make this cut. Three Milwaukee hole saws were machined in necessary places and then welded together to form one long hole saw (Figure 66). This hand-made tool was successful in making the cut through the wall without touching the pipes connected to the heating element (Figure 67). This allowed the heating element to then be able to come out of the autoclave, and the remaining material of the insulated wall that clung around the pipes was cut off with an angle grinder.

Figure 66: Custom tool made for repairing of autoclave

Figure 67: Heating element removed from autoclave

Now a repair was to be made to the structure, as permanent damage was done. The wall contains a fiberglass insulation, held in place by material similar to chicken wire and sandwiched

between two aluminum walls, the first almost half an inch thick, with the other being much thinner. It is important to note that the insulation was isolated from the chamber pressure because when pressure comes into contact with fiberglass, it gets compressed and loses its effectiveness for thermal insulation. Another important aspect is the original size of the hole. Two half inch outer diameter pipes went through the insulated wall via 0.75" inner diameter holes that sealed off the insulation. This dimension would be critical, in that all mass air flow into the curing chamber goes through these two holes. It would also be important to maintain the original manufacturer specifications to minimize the hot air allowed back in past the insulation wall, as that area houses a fan that must be kept cool.

The solution was to fill the hole with a 1.5" threaded rod with the center 1.0625" bored out to allow for the pipes and fittings to pass through their holes. On each end of the rod would be a washer and two nuts compressing high temperature JB Weld putty that would help to seal off the insulation from the pressurized chamber. On the side of the wall where the fittings were present, two aluminum inserts would wrap around each pipe and press into the bored threaded rod to allow for air flow that was choked to the manufacturer specifications, having an inner diameter of 0.75" (Figure 68).

Figure 68: Repair of Autoclave

Once the repair was made, wiring was redone, and all components were set back in place, the autoclave was tested and found to be in full working order. Fabrication of the double lap joint samples was then able to continue. In an attempt to make up for time lost while the autoclave was down, an increased rate of fabrication was introduced, using a bigger aluminum plate than before as a tool. This new plate was cut to 17.5" by 30" and would allow for four samples to be made in one panel. Due to the width of the plate and the bottom table in the autoclave only being able to support plates that are 12" wide, 2" x 2" square stock steel tubing pieces were cut to length and used as risers of the bottom table of the autoclave. Cutting of this panel was not the easiest task, as the X and Y dimensions of the panel both surpassed the limitations of the cutting head and completely covered the cutting table (Figure 69). Overall, this attempt at an increase in production rate was successful, as the autoclave and waterjet machines could be used to their full capacities.
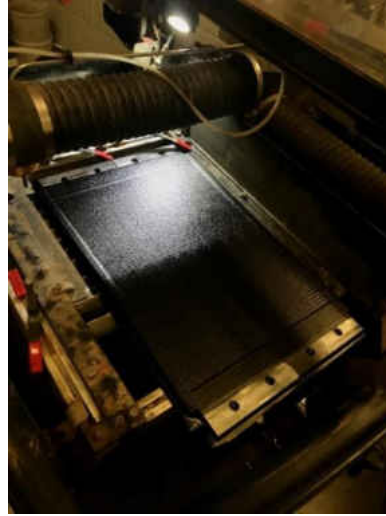
(a)   (b)

Figure 69: Fabrication of DLJ large panel: (a) autoclave curing and (b) waterjet cutting

The testing plan is shown in Figure 70, as samples with and without through thickness reinforcement were manufactured. For the TTR reinforced samples, 4 rows of holes were drilled in a 5mm spaced grid pattern, starting approximately 5mm away from the gap. The same methods were used in this process as in the four-point bending samples; however, both sides of the double lap joint samples were reinforced as opposed to one side. The reasoning for this is due to the symmetry in the geometry of the sample and the stresses that occur on both sides.

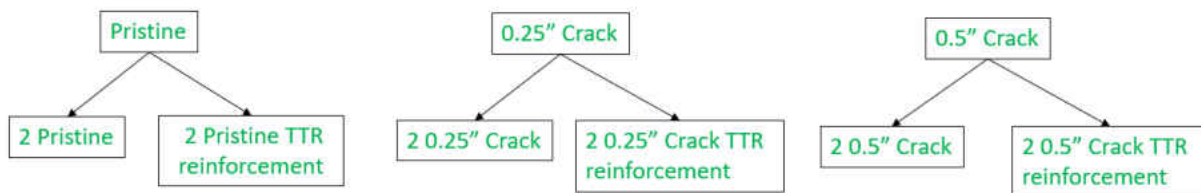*Figure 70: Fabrication and testing plan for double lap joint samples*

As for the testing of the autoclave cured samples, experimentation went flawlessly. All of these samples broke where expected (at the double lap joint), rather than failing prematurely and at the wrong location. The same testing setup was used as displayed in Figure 58. Further discussion with regard to testing will be discussed in the results section.

DOUBLE LAP JOINT RESULTS

In NASA's study of this configuration of joining two composite structures together, a result that was five times the design limit was obtained before failure of their samples. The idea of a double lap joint method had been proven already; however, the addition of through thickness reinforcement had not been applied to this design. The results of this experiment primarily look into the possible enhancement of loading characteristics and suppression of crack propagation in a double lap joint sample design loaded in tension.

Due to NASA's difference in layup design, materials, and number of plies, the baseline of this experiment is of the pristine sample design mentioned earlier in the methods section. All successful samples were cured in the autoclave, as panel A was cured in the heat press and had failure in the adaptor ends, as they pulled out prematurely. Panel C also experienced fabrication issues, as the adaptor ends were cured in a mis-aligned manner. Table 7 and Figures 71, 72, and 73 show the data obtained from the pristine samples and images of the corresponding samples. The data in red is rejected due to its defects obtained in the manufacturing process.

Table 7: Double Lap Joint Tension – Pristine Data

Pristine			
Sample	Maximum Load (lbf)	Stiffness (lbf/in)	Failure Type
TB1	14168	88444	Net Section Failure
TB2	15680	89283	Net Section Failure
TC1	11924	105800	Net Section Failure
TC2	10967	103720	Net Section Failure
Average	13185	96812	
Accepted Average	14924	88864	
Standard Deviation	756	420	
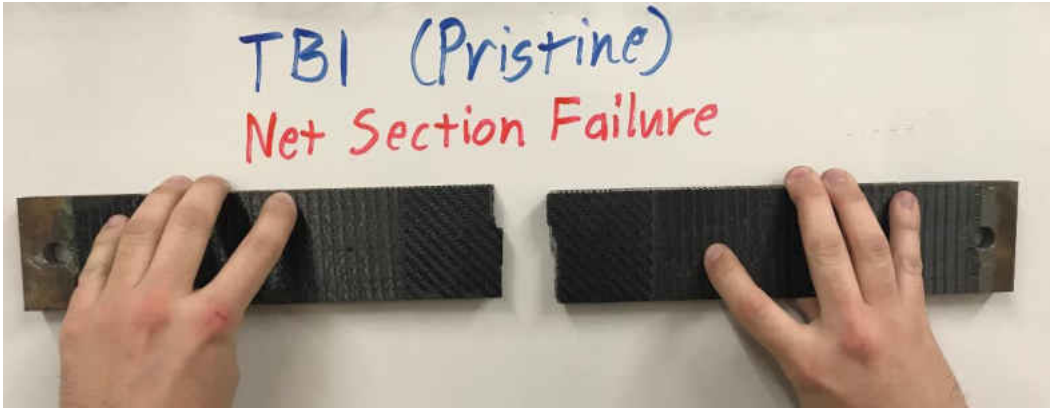
Figure 71: Failure of a double lap joint pristine sample (front)

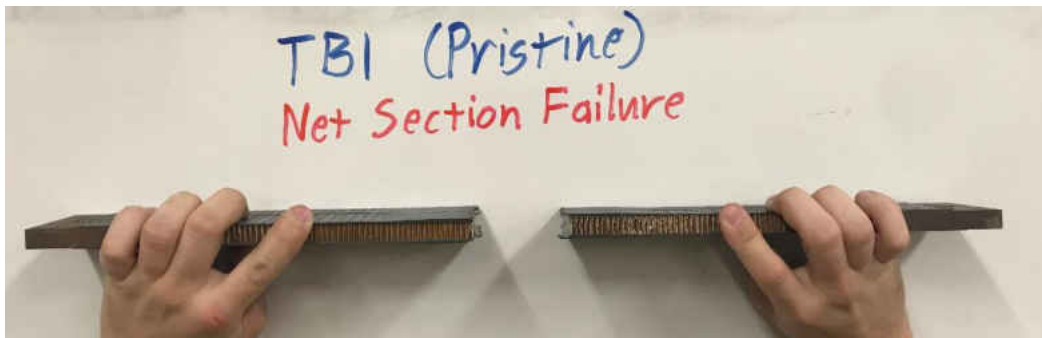*Figure 72: Failure of a double lap joint pristine sample (side)*

Figure 73: Misalignment of the end adaptor in sample TC2

Following the pristine samples, panels with a 1/4" crack between the fifth and sixth facesheet plies at the joint were fabricated and tested. Some samples would be reinforced with rows of through thickness reinforcement while others would be tested non-reinforced and

containing the defect. When loaded, some non-reinforced samples showed crack propagation while others had a net section failure similar to that of the pristine samples. The samples with the TTR reinforcement showed signs of crack propagation up to the first row of inserted rods. Failure load values were noticeably lower than the non-defected samples. Stiffness also changed but in the other direction than expected. See the table and figures below for 1/4" crack double lap joint sample data and images.

Table 8: Double Lap Joint Tension – 1/4" Teflon Crack Defect Data

1/4" Teflon Crack			
Sample	**Maximum Load (lbf)**	**Stiffness (lbf/in)**	**Failure Type**
TD1	13623	105696	Net Section Failure
TD2	10037	109592	Net Section Failure
TE1	13566	104392	Mixed Failure Type
TE2	13750	104395	Major Delamination
Average	12744	106019	
Accepted Average	13646	104828	
Standard Deviation	77	614	
% Difference to Pristine	-8.6%	18.0%	

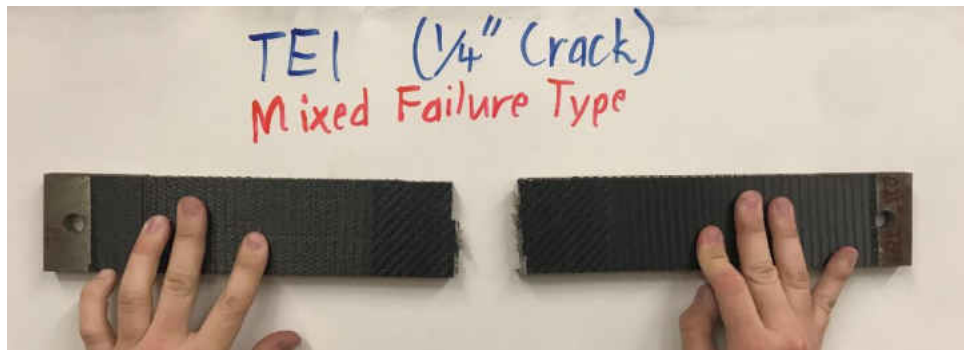| 1/4" Teflon Crack with TTR			
Sample	**Maximum Load (lbf)**	**Stiffness (lbf/in)**	**Failure Type**
TF1	13103	103029	Prevented Delamination
TF2	11666	103627	Prevented Delamination
Average	12384	103328	
Standard Deviation	718	299	
% Difference to 1/4" Crack	-9.2%	-1.4%	

Figure 74: Mixed mode of failure of a double lap joint 1/4" defect sample (front view)
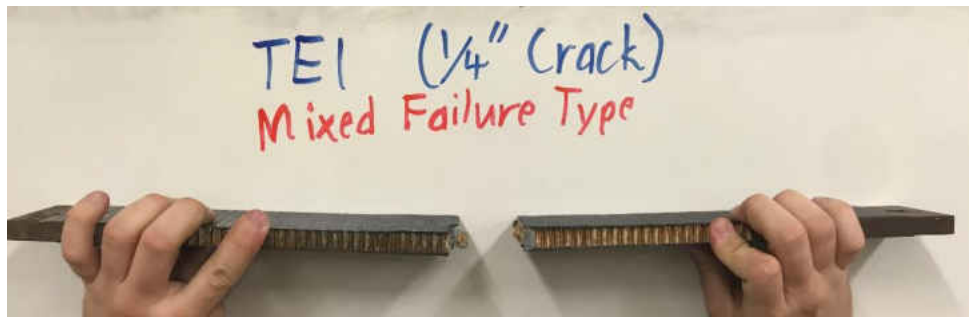

Figure 75: Mixed mode of failure of a double lap joint 1/4" defect sample (side)

Figure 76: Crack propagation failure of a double lap joint 1/4" defect sample (front)

Figure 77: Crack propagation failure of a double lap joint 1/4" defect sample (side)

Figure 78: Prevented delamination of a double lap joint 1/4" defected sample (front)

Figure 79: Prevented delamination of a double lap joint 1/4" defected sample (side)

In order to improve the chances of crack propagation and of the prevention of crack propagation through use of TTR, a 1/2" crack defect sample design was deemed to be necessary.

All non-reinforced 1/2" crack defected samples showed major crack propagation. Furthermore, signs of prevented crack propagation were present in the TTR reinforced 1/2" crack defected samples. Further knockdown in load capacity and a fairly constant stiffness were observed when compared to the 1/4" crack defected samples with and without TTR reinforcement. The recorded data and images of the failure types for these samples are in the table and figures below.

Table 9: Double Lap Joint Tension Data – 1/2" Teflon Crack Defect Data

1/2" Teflon Crack			
Sample	**Maximum Load (lbf)**	**Stiffness (lbf/in)**	**Failure Type**
TG1	11297	101470	Major Delamination
TG2	12513	101045	Major Delamination
Average	11905	101258	
Standard Deviation	608	213	
% Difference to Pristine	-20.2%	13.9%	

1/2" Teflon Crack with TTR			
Sample	**Maximum Load (lbf)**	**Stiffness (lbf/in)**	**Failure Type**
TG3	12787	100212	Prevented Delamination
TG4	11999	92214	Prevented Delamination
Average	12393	96213	
Standard Deviation	394	3999	
% Difference to 1/2" Crack	4.1%	-5.0%	

Figure 80: Crack propagation failure of a double lap joint 1/2" defect sample (front)

Figure 81: Crack propagation failure of a double lap joint 1/2" defect sample (side)
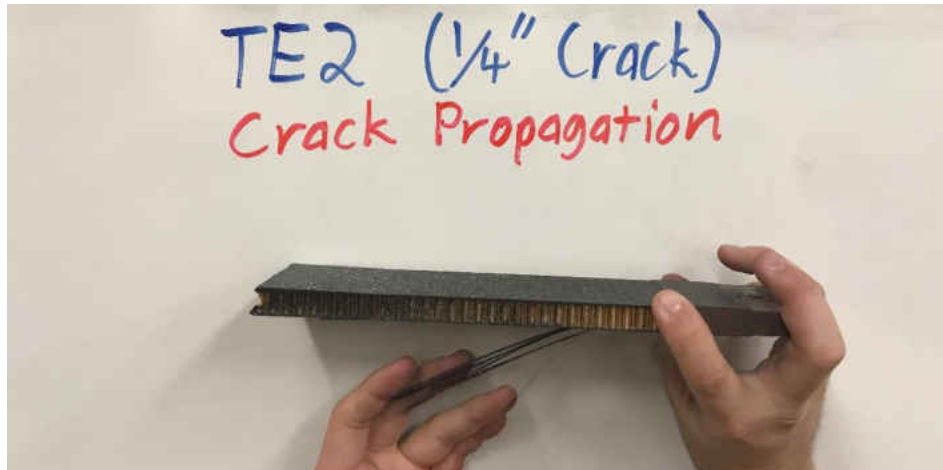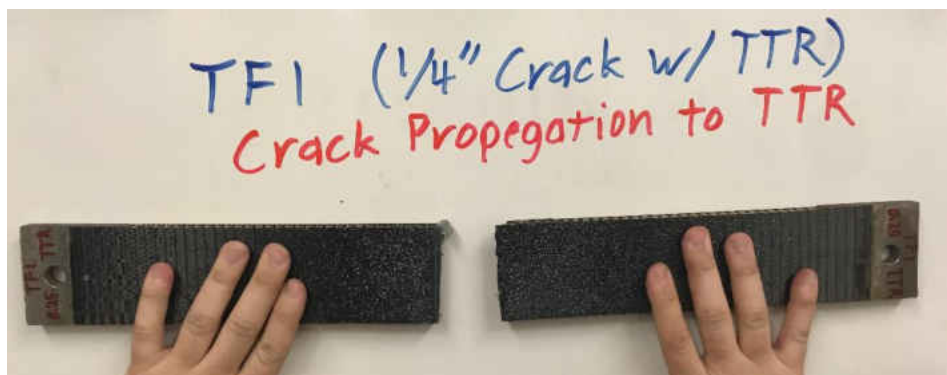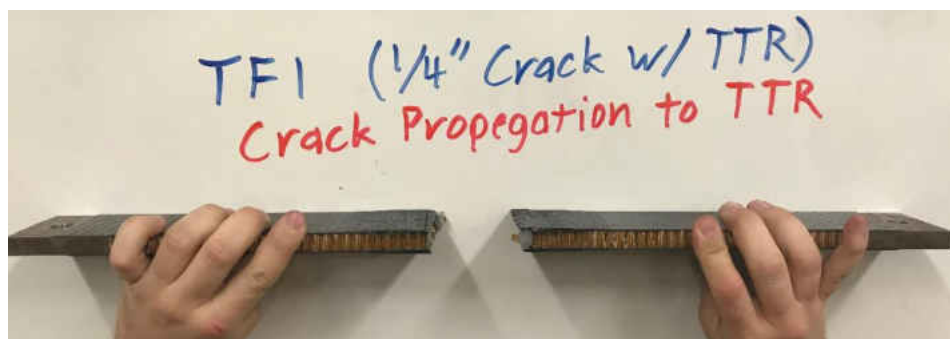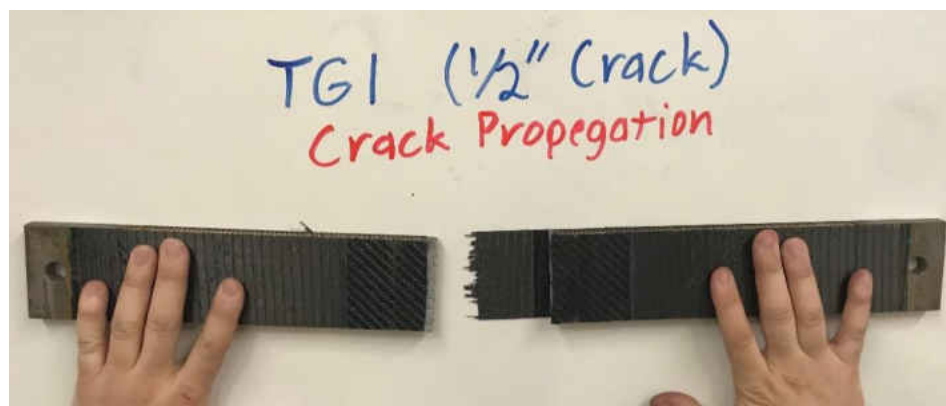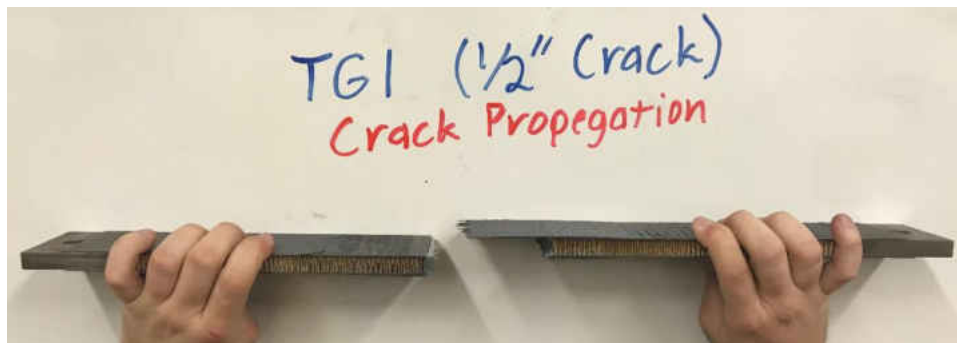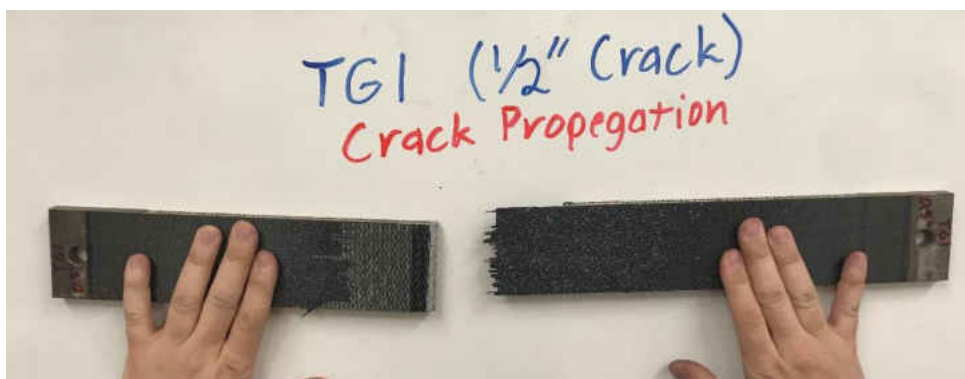

Figure 82: Crack propagation failure of a double lap joint 1/2" defect sample (back)
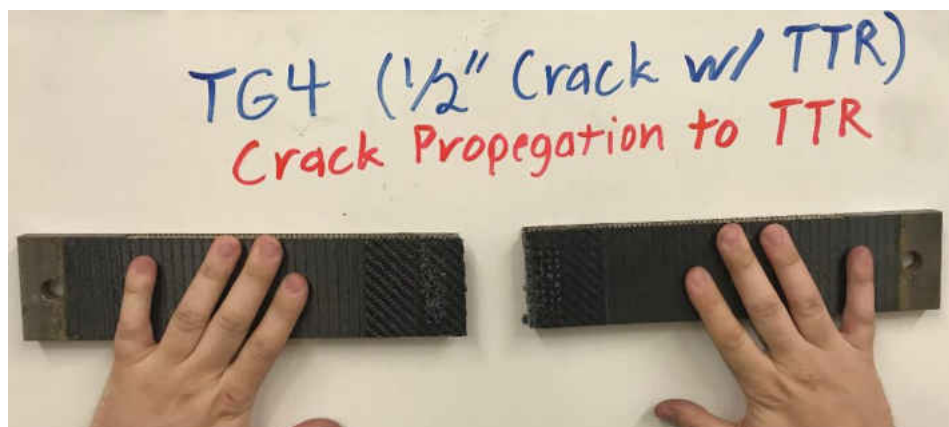
Figure 83: Prevented delamination of a double lap joint 1/2" defected sample (front)
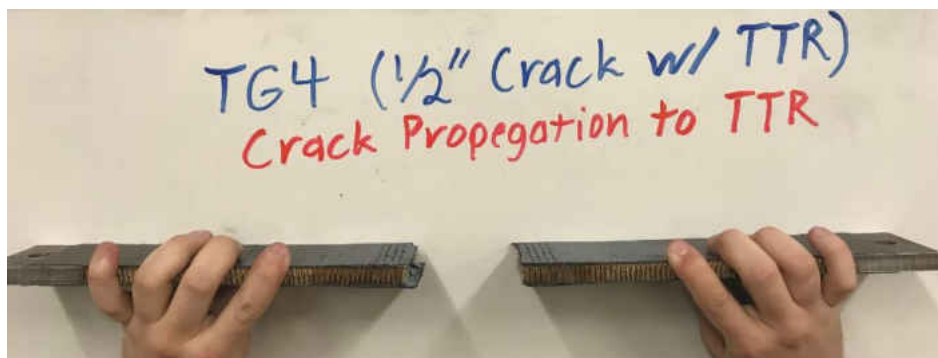
Figure 84: Prevented delamination of a double lap joint 1/2" defected sample (side)

When combining the loading data together across all sample types, Figures 85 and 86 are obtained. In the load vs displacement graphs, a small deviation in the stiffness among samples is shown, in addition to the differing peak load values. The bar chart displays the average failure loading values of each group of samples, along with their standard deviations.
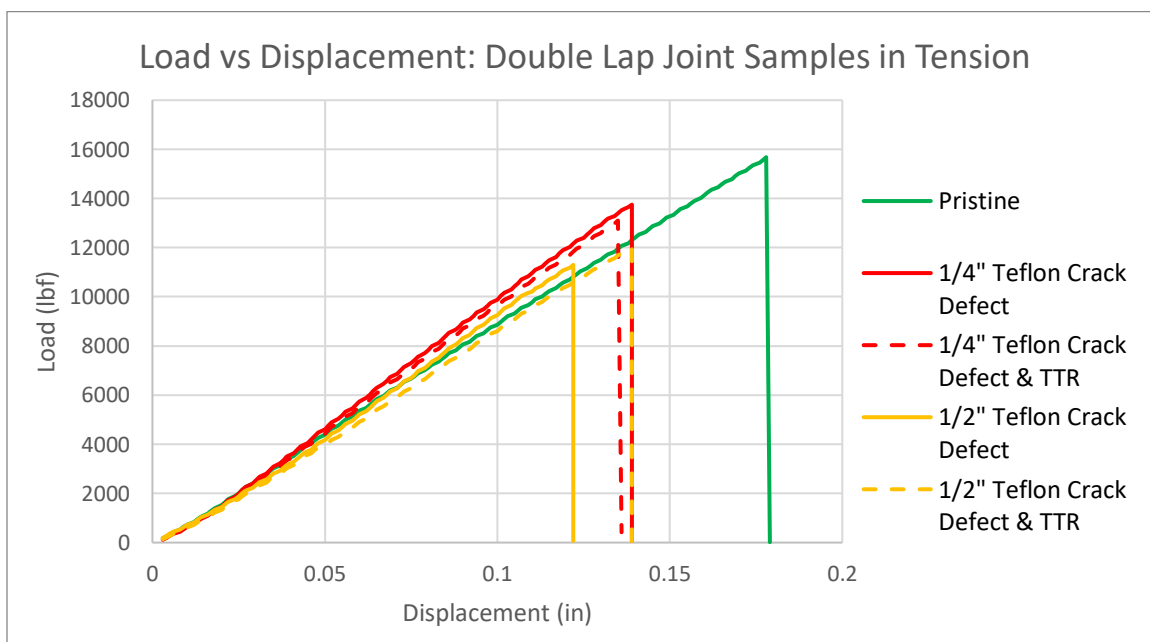
Figure 85: Load vs displacement curves for double lap joint samples

Figure 86: Bar chart load comparison of double lap joint samples with standard deviations

DOUBLE LAP JOINT DISCUSSION

To briefly speak to the performance of TTR on double lap joints, there were pros and cons of this method. In regard to the pros, crack propagation was suppressed and the manufacturability of the reinforced double lap joint was proven. Some cons include the extra time and effort involved in reinforcement of the area surrounding the joint and in the lack of adding any additional load carrying capabilities.
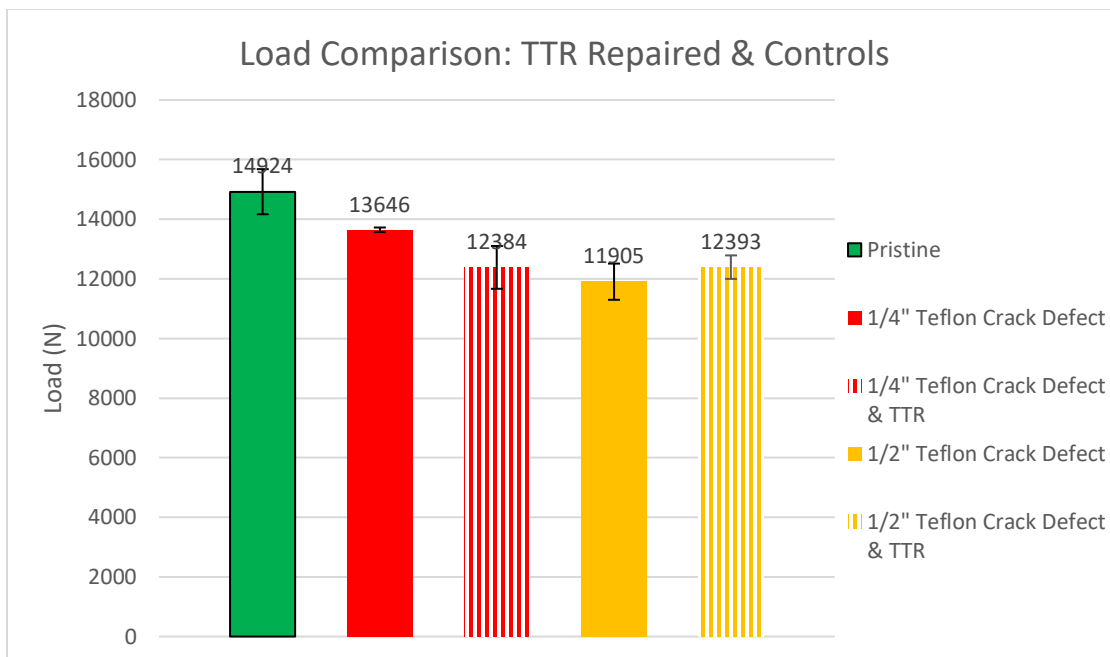
Overall, a general downward trend in failure loads was observed, as seen in Figure 87. One outlier of this trend was in the 1/2" teflon crack defected samples, as the average seemed to be on par with that of the 1/4" teflon crack defected samples. Further investigation using another crack length would be worthwhile in proving whether this was an anomaly or the TTR helps to prevent further knockdown in loading capacity.

Another observation that was not expected was in the deviation of stiffnesses among the sample types. This may be due to the manufacturing of multiple batches, as NASA's approach in the manufacturing of one panel for all samples in a larger autoclave would be a more ideal route.

When looking at the strain images, a few interesting findings came from the DIC. Figures 87 through 91 show the visualized strain for all different sample types in this study. Prior to failure of the pristine sample, the strain appears to build up on each side of the 0.1" gap. This could be explained by the sudden geometry changes that occur in this region and how the sample goes from ten plies of thickness to four and back to 10 at this joint section.
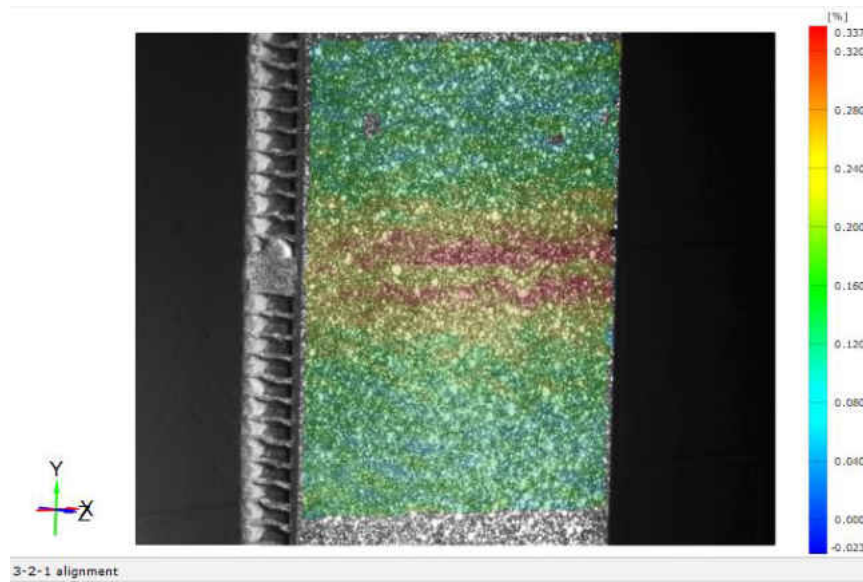
Figure 87: DIC strain image a pristine DLJ sample

Figure 88: DIC strain image of a DLJ sample with a 1/4" delamination before failure

Figure 89: DIC strain image of a DLJ sample with a 1/4" delamination and TTR before failure

In Figures 88 and 89, a comparison between double lap joint samples with a 1/4" defect can be made.
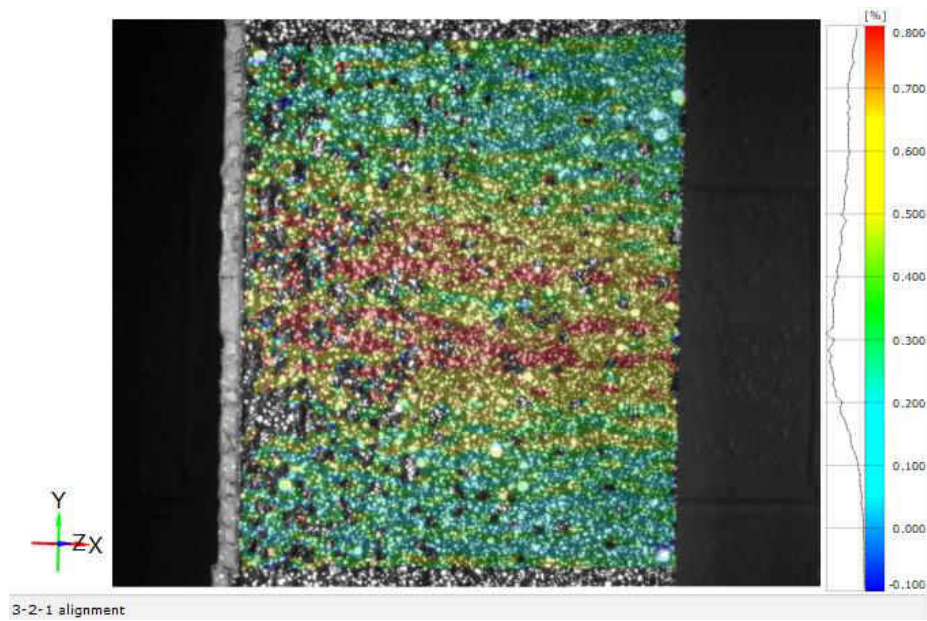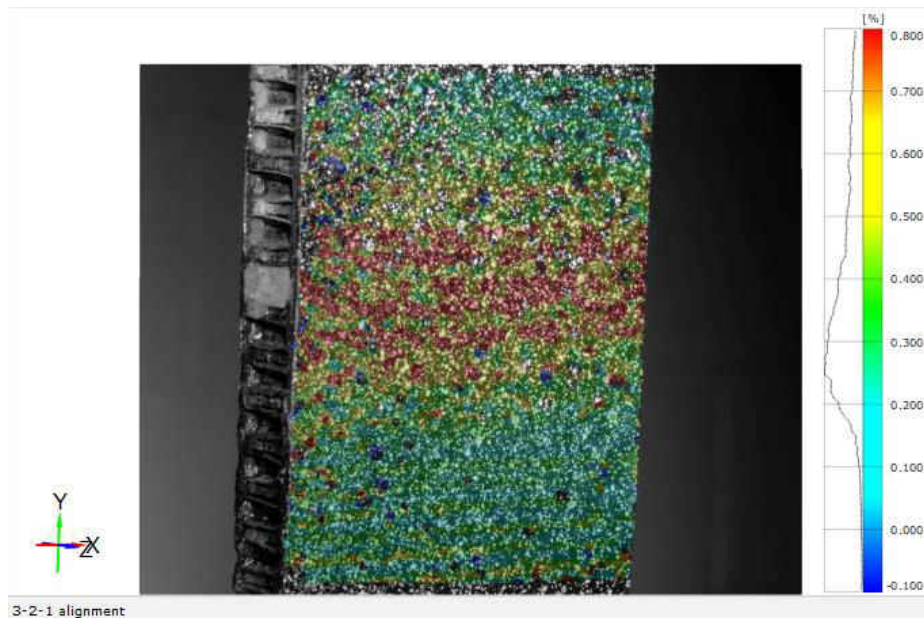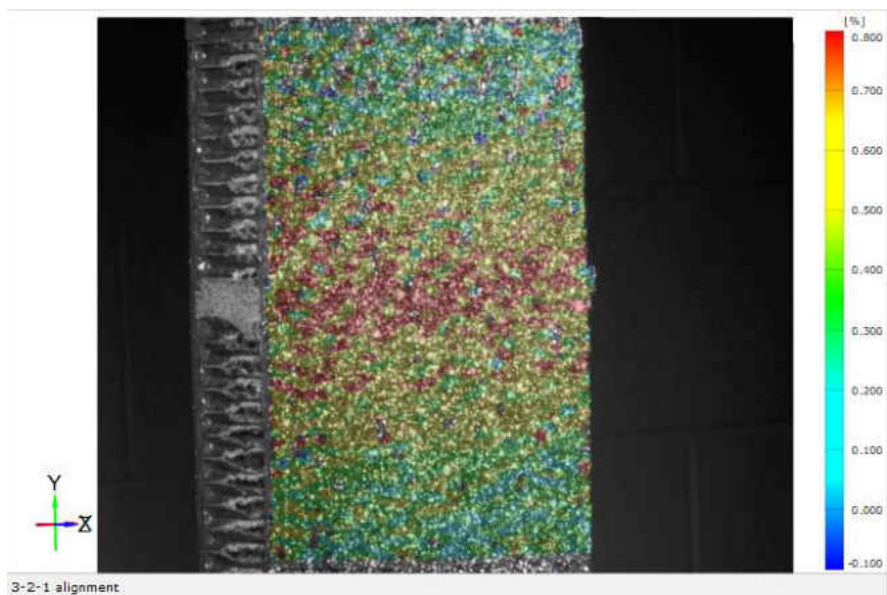

Figure 90: DIC strain image of a DLJ sample with a 1/2" delamination before failure

Figure 91: DIC strain image of a DLJ sample with a 1/2" delamination and TTR before failure

CONCLUSIONS

The use and the effectiveness of through thickness reinforcement (TTR) in four-point bending samples not only was brought up in Mr. Suresh's experimentation but also was further proven in this study. TTR is an excellent method of repair and reinforcement for composite honeycomb structures, especially when exerted to the composite's limits in four-point bending. Not only is a higher failure load achieved, but a higher allowed displacement before structure failure is obtained. While a confident conclusion in the increase of TTR effectiveness as a function of the increase in facesheet thickness cannot be determined at this point, the data was certainly steering that way. Further experimentation using this design for the delaminated samples or with a new core would be recommended for future work.

As for the use of TTR in adhesively bonded joints when loaded in tension, the reinforcement was helpful in isolating the damage to the weaker part of the structure and preventing delamination across the facesheet. TTR proved only to be good in suppressing crack growth and added no additional loading capabilities to the structure.

REFERENCES

[1] N. Gromicko, "The History of Concrete," *International Association of Certified Home Inspectors*. [Online]. Available: https://www.nachi.org/history-of-concrete.htm#ixzz31V47Zuuj. [Accessed: 14-Jan-2020].

[2] Y. Deng, "CARBON FIBER ELECTRONIC INTERCONNECTS," University of Maryland, College Park, MD, 2007.

[3] R. Millington and R. Nordberg, "PROCESS FOR PREPARING CARBON FIBERS," 3,294,489, 27-Dec-1966.

[4] "Stand Points," *FLIGHT International*, p. 481, 26-Sep-1968.

[5] D. E. Hartz, D. G. Erickson, and W. B. Hopkins, "(54) COMPOSITE HONEYCOMB SANDWECH STRUCTURE," 5604010, 18-Feb-1997.

[6] G. Kim, T. Futch, R. Sterkenburg, S. Ahsan, G. Kilaz, and B. Kozak, "Investigating The Effects of Fluid Intrusion on Nomex® Honeycomb Structures with Carbon Fiber Face Sheets," p. 13, 2017.

[7] M. Okur, S. Kangal, and M. Tanoğlu, *Development of Aluminum Honeycomb Cored Carbon Fiber Reinforced Polymer Composite Based Sandwich Structure*. 2018.

[8] Z. Kolakowski, "On some aspects of the modified TSAI-WU criterion in thin-walled composite structures," *Thin-Walled Struct.*, vol. 41, no. 4, pp. 357–374, Apr. 2003, doi: 10.1016/S0263-8231(02)00112-X.

[9] A. Ural, A. T. Zehnder, and A. R. Ingraffea, "Fracture mechanics approach to facesheet delamination in honeycomb: measurement of energy release rate of the adhesive bond," *Eng. Fract. Mech.*, vol. 70, no. 1, pp. 93–103, Jan. 2003, doi: 10.1016/S0013-7944(02)00024-3.

[10] J. Childress and G. Freitas, "z-direction pinning of composite laminates for increased survivability," in *Aerospace Design Conference*, Irvine,CA,U.S.A., 1992, doi: 10.2514/6.1992-1099.

[11] D. Cartie, G. Dell'Anno, E. Poulin, and I. Partridge, "3D reinforcement of stiffener-to-skin T-joints by Z-pinning and tufting," *Eng. Fract. Mech.*, vol. 73, no. 16, pp. 2532–2540, Jun. 2006, doi: 10.1016/j.engfracmech.2006.06.012.

[12] S. Kravchenko, O. Kravchenko, M. Wortmann, M. Pietrek, P. Horst, and R. B. Pipes, "Composite toughness enhancement with interlaminar reinforcement," *Compos. Part Appl. Sci. Manuf.*, vol. 54, pp. 98–106, Nov. 2013, doi: 10.1016/j.compositesa.2013.07.006.

[13] S. G. Kravchenko, O. G. Kravchenko, L. A. Carlsson, and R. B. Pipes, "Influence of through-thickness reinforcement aspect ratio on mode I delamination fracture resistance," *Compos. Struct.*, vol. 125, pp. 13–22, Jul. 2015, doi: 10.1016/j.compstruct.2015.01.032.

[14] M. Suresh, A. Sanders, P. Prajapati, K. Kaipa, and O. Kravchenko, "COMPOSITE SANDWICH REPAIR USING THROUGH-THICKNESS REINFORCEMENT WITH ROBOTIC HAND MICRO-DRILLING," in *Dropbox*, Novi, MI, 2019.

[15] B. H. Mason, A. Satyanarayana, and D. W. Sleight, "Test and Analysis Correlation for Sandwich Composite Longitudinal Joint Specimens," in *AIAA Scitech 2019 Forum*, San Diego, California, 2019, doi: 10.2514/6.2019-0235.

[16] L. F. M. da Silva and R. D. S. G. Campilho, "2 - Design of adhesively-bonded composite joints," in *Fatigue and Fracture of Adhesively-Bonded Composite Joints*, A. P. Vassilopoulos, Ed. Woodhead Publishing, 2015, pp. 43–71.

[17] H. Bendemra, P. Compston, and P. J. Crothers, "Optimisation study of tapered scarf and stepped-lap joints in composite repair patches," *Compos. Struct.*, vol. 130, pp. 1–8, Oct. 2015, doi: 10.1016/j.compstruct.2015.04.016.

[18] I. Daniel and O. Ishai, *Engineering Mechanics of Composite Materials*, 2nd edition. Oxford University Press, 2006.

[19] Fibre Glast Developments Corporation, "Prepreg 4.3 oz IM Unidirectional Fabric 6-Month - Product Data Sheet." .

[20] Henkel Corporation Aerospace, "LOCTITE EA 9696 AERO - Material Data Sheet." Sep-2013.

[21] J. Wang, C. Shi, N. Yang, H. Sun, Y. Liu, and B. Song, "Strength, stiffness, and panel peeling strength of carbon fiber-reinforced composite sandwich structures with aluminum honeycomb cores for vehicle body," *Compos. Struct.*, vol. 184, pp. 1189–1196, Jan. 2018, doi: 10.1016/j.compstruct.2017.10.038.

[22] Z. Sun, S. Shi, X. Guo, X. Hu, and H. Chen, "On compressive properties of composite sandwich structures with grid reinforced honeycomb core," *Compos. Part B Eng.*, vol. 94, pp. 245–252, Jun. 2016, doi: 10.1016/j.compositesb.2016.03.054.

[23] Plascore Corporation, "PN2 Aerospace Grade Aramid Fiber Honeycomb - Material Data Sheet." .

[24] M. D. Banea and L. F. M. da Silva, "Adhesively bonded joints in composite materials: An overview," *Proc. Inst. Mech. Eng. Part J. Mater. Des. Appl.*, vol. 223, no. 1, pp. 1–18, Jan. 2009, doi: 10.1243/14644207JMDA219.

[25] H. M. Hsiao, S. M. Lee, and R. A. Buyny, "Core Crush Problem in the Manufacturing of Composite Sandwich Structures: Mechanisms and Solutions," *AIAA J.*, vol. 44, no. 4, pp. 901–907, Apr. 2006, doi: 10.2514/1.18067.

VITA

Aleric Alden Sanders

EDUCATION

Master of Science in Mechanical Engineering at Old Dominion University, August 2018 – Present, Norfolk, Virginia. Thesis title: "Through-Thickness Reinforcement and Repair of Carbon Fiber Based Honeycomb Structures under Flexure and Tension of Adhesively Bonded Joints"

Bachelor of Science in Mechanical Engineering at Old Dominion University, Norfolk, Virginia, August 2014 – May 2018.

ACADEMIC EMPLOYMENT

Undergraduate Research Assistant, Department of Mechanical and Aerospace Engineering, Old Dominion University, August 2017 – May 2018

Graduate Teaching Assistant, Department of Mechanical an Aerospace Engineering, Old Dominion University, August 2018 – December 2019

PROFESSIONAL EXPERIENCE

Manufacturing Engineering Internship at STIHL Inc., Virginia Beach, Virginia, summer of 2018. Responsibilities included: Solidworks modeling, machine testing, machine improvement, and testing of materials.

Product Support Internship at Volvo Penta of the Americas, Chesapeake, Virginia, summers of 2016 and 2017. Responsibilities included: Communications and problem solving with Volvo Penta dealers, technicians, and customers involving repair and maintenance of marine and industrial Volvo Penta equipment.

PRESENTATIONS AT PROFESSIONAL MEETINGS

M. Suresh, A. Sanders, and Dr. O. Kravchenko. Through Thickness Reinforcement and Repair of Composite Sandwich Structures. 2019 Society of Petroleum Engineers (SPE) Automotive Composites Conference & Exhibition (ACCE), Novi, Michigan, September 4-6, 2019

PROFESSIONAL MEMBERSHIPS

Society of Automotive Engineers (SAE) May 2014 – Present.

Involvement with Old Dominion University's Formula SAE organization August 2014 – May 2018.